

**USE OF ACID MINE DRAINAGE IN RECYCLING OF MARCELLUS SHALE
FLOWBACK WATER: SOLIDS REMOVAL AND POTENTIAL FOULING OF
POLYMERIC MICROFILTRATION MEMBRANES**

by

Xuhan Wang

B.S. in Water and Wastewater Engineering, South China University of Technology, China, 2010

Submitted to the Graduate Faculty of

Swanson School of Engineering in partial fulfillment

of the requirements for the degree of

Master of Science in Civil Engineering

University of Pittsburgh

2012

UNIVERSITY OF PITTSBURGH
SWANSON SCHOOL OF ENGINEERING

This thesis was presented

by

Xuhan Wang

It was defended on

March 29, 2012

and approved by

Radisav D. Vidic, PhD, Professor, Department of Civil and Environmental
Engineering

Leonard W. Casson, PhD, Associate Professor, Department of Civil and Environmental
Engineering

Jason D. Monnell, PhD, Research Assistant Professor, Department of Civil and
Environmental

Thesis Advisor: Radisav D. Vidic, PhD, Professor, Department of Civil and Environmental
Engineering

Copyright © by Xuhan Wang

2012

**USE OF ACID MINE DRAINAGE IN RECYCLING OF MARCELLUS SHALE
FLOWBACK WATER: SOLIDS REMOVAL AND POTENTIAL FOULING OF
POLYMERIC MICROFILTRATION MEMBRANES**

Xuhan Wang, M.S.

University of Pittsburgh, 2012

Flowback water generated by hydraulic fracturing during shale gas reservoir stimulation can be reused for subsequent fracturing process. Acid mine drainage (AMD) is a potential water source that could alleviate low flowback water recovery by serving as a makeup water. AMD located near gas wells can be mixed with flowback water (Mixture 1 and 2), resulting in precipitation of barium sulfate. The feasibility of microfiltration to separate solids from two sets of mixtures of AMD and flowback water was evaluated using a bench-scale set-up. Hydrophilic polyvinylidene fluoride (PVDF) membranes with a pore size of 0.22 μm were used in the experiments.

Severe membrane fouling occurred early during Mixture 1 filtration, while no significant fouling occurred for Mixture 2. Particle size distribution analysis and fouling mechanism identification of the two mixtures were performed to understand the cause of membrane fouling.

The dominant fouling mechanisms in the early stages of Mixture 1 filtration were standard blocking (pore constriction) and complete blocking (pore blocking) caused by particles in the flowback water with size in the range of membrane pore diameter. On the contrary, no significant standard blocking or complete blocking was found during the filtration of Mixture 2, which was due to the fact that most particles in Flowback water B or Mixture 2 were larger than the membrane pore diameter.

Additional filtration experiments were conducted using two barium sulfate solutions containing an order of magnitude difference in precipitate concentration. Identical permeate flux behavior were observed in both experiments. Therefore, precipitated had limited impact on membrane fouling.

As an alternative to membrane filtration, coagulation with aluminium chloride and ferric chloride followed by sedimentation was investigated for turbidity and total organic carbon (TOC) removal. Ferric chloride dosage of 30mg/L at pH=6 for Mixture 1 and 20mg/L at pH=6 for Mixture 2 were found to be optimal coagulation parameters that could achieve similar turbidity and TOC removal (around 90%) as membrane filtration.

This study has shown that membrane filtration has the potential to replace conventional coagulation – flocculation – sedimentation process for flowback water treatment for solids removal, but its efficiency depends on the flowback water quality.

Keywords: Marcellus Shale, Flowback water, Acid mine drainage (AMD), Microfiltration, Barium sulfate, Coagulation - flocculation

TABLE OF CONTENTS

ACKNOWLEDGMENTS	XI
1.0 INTRODUCTION.....	1
2.0 LITERATURE REVIEW.....	4
2.1 FLOWBACK WATER	4
2.1.1 Flowback water disposal.....	4
2.1.2 Flowback water disposal regulation	5
2.2 AMD POLLUTION AND REGULATIONS.....	5
2.3 SUSTAINABLE METHODS TO TREAT FLOWBACK WATER	6
2.4 MEMBRANE FILTRATION.....	7
2.5 PROCESS PARAMETERS.....	7
2.5.1 Permeate flux	8
2.5.2 Permeability coefficient.....	8
2.5.3 Volume concentration factor	9
2.6 FOULING MECHANISM THEORY.....	9
3.0 MATERIALS AND METHODS	12
3.1 FEED WATER.....	12
3.1.1 Feed water collection and preparation	12
3.1.2 Feed water	17

3.2	PARTICLE SIZE DISTRIBUTION	18
3.3	TOC.....	18
3.4	DEAD-END MEMBRANE FILTRATION.....	19
3.5	COAGULATION AND FLOCCULATION	20
4.0	RESULTS AND DISCUSSION	23
4.1	MEMBRANE FILTRATION.....	23
4.1.1	Particle size distribution	23
4.1.2	Permeate flux behavior	27
4.1.3	Fouling mechanism identification	34
4.2	COAGULATION AND FLOCCULATION	50
5.0	SUMMARY AND CONCLUSIONS	56
6.0	RECOMMENDATIONS FOR FUTURE WORK.....	58
	APPENDIX A	59
	APPENDIX B	76
	APPENDIX C	80
	BIBLIOGRAPHY	83

LIST OF TABLES

Table 1. Fouling mechanisms and their corresponding physical basis (Grenier et. al., 2008)	11
Table 2. Composition of the flowback water composite: Flowback water A and Flowback water B	15
Table 3. Flowback and AMD water characteristics	17
Table 4. Coagulant dose and pH conditions tested	22
Table 5. Barium sulfate concentration in Sample 1 and 2	33
Table 6. Fouling mechanism identification data summary for flowback water and AMD	46
Table 7. Initial turbidity, particle size distribution data summary for flowback water and AMD	47
Table 8. Cake volumic specific resistance, blocking parameter data summary for flowback water and AMD	49
Table 9. Summary of turbidity and TOC removal by coagulation-flocculation-sedimentation ...	54
Table 10. Summary of optimal coagulant dosages	55
Table 11. Summary of turbidity removed through precipitation, membrane filtration and coagulation - flocculation	55

LIST OF FIGURES

Figure 1. Flowback water flowrate and water recovery for the site A (arrows mark days when the samples were collected).....	13
Figure 2. Flowback water flowrate and water recovery for the site B.....	14
Figure 3. Experimental dead-end membrane filtration apparatus.....	20
Figure 4. Particle size distribution measured using Microtrac S3500: Flowback water A.....	24
Figure 5. Particle size distribution measured using Microtrac S3500: Flowback water B.....	25
Figure 6. Particle size distribution measured using Microtrac S3500: Mixture 1	26
Figure 7. Particle size distribution measured using Microtrac S3500: Mixture 2	27
Figure 8. Permeate flux vs. time for Mixture 1 and Mixture 2.....	28
Figure 9. Permeate flux vs. VCF for Mixture 1, diluted Flowback water A and diluted AMD 1	29
Figure 10. Permeate flux vs. VCF for Mixture 2, diluted Flowback water B and diluted AMD 2	30
Figure 11. Permeate flux vs. VCF for diluted Flowback water A and Flowback water B.....	31
Figure 12. Permeate flux vs. VCF for diluted AMD 1 and diluted AMD 2	32
Figure 13. Permeate flux vs. VCF for Sample 1 and Sample 2.....	34
Figure 14. Fouling mechanism identification for the Mixture 1: Standard blocking	36
Figure 15. Fouling mechanism identification for the Mixture 1: Complete blocking	37
Figure 16. Particle size distribution measured using Malvern Zetasizer: Flowback water A	38
Figure 17. Fouling mechanism identification for the Mixture 1: Cake filtration	39
Figure 18. Fouling mechanism identification for the Mixture 1: Intermediate blocking	40

Figure 19. Fouling mechanism identification for the Mixture 2: Standard blocking	41
Figure 20. Fouling mechanism identification for the Mixture 2: Complete blocking	42
Figure 21. Fouling mechanism identification for the Mixture 2: Cake filtration	43
Figure 22. Fouling mechanism identification for the Mixture 2: Intermediate blocking	44
Figure 23. Residual turbidity and TOC as a function of iron dose for Mixture 1 (initial turbidity = 33 NTU, initial TOC = 2.4 mg/L)	51
Figure 24. Residual turbidity and TOC as a function of aluminium dose for Mixture 1 (initial turbidity = 33 NTU, initial TOC = 2.4 mg/L)	52
Figure 25. Residual turbidity and TOC as a function of iron dose for Mixture 2 (initial turbidity = 4.9 NTU, initial TOC = 5.0 mg/L)	53
Figure 26. Residual turbidity and TOC as a function of aluminium dose for Mixture 2 (initial turbidity = 4.9 NTU, initial TOC = 5.0 mg/L)	54

ACKNOWLEDGMENTS

I would like to acknowledge all people that contributed to the accomplishment of this research. Dr. R.D. Vidic for his support and guidance. Dr. J.D. Monnell and Dr. L.W. Casson for their advice and suggestion. Dr. E. Barbot for her advice and laboratory assistance. And my family and friends for their love and support.

1.0 INTRODUCTION

Natural gas contained in various shale formations around the world represents an important energy source that is projected to continue its growth in the future (EIA, 2011). Recent report by the US Energy Information Administration (EIA, 2011) indicated that over 860 trillion cubic feet (tcf) of technically recoverable natural gas is available in the United States. The Marcellus Shale formation that lies from upstate New York, as far south as Virginia, and as far west as Ohio, covering 70% of the surface of Pennsylvania is one of the largest shale gas reservoirs in the US with an estimated 262-500 tcf of natural gas reserves (Milici and Swezey, 2006; Engelder and Lash, 2008).

Horizontal drilling and hydraulic fracturing are the key technologies that enable economic recovery of this natural resource (King, 2010; Reinicke et al., 2010). Hydraulic fracturing involves the injection of fracturing fluid and proppant under high pressure to create a network of fractures that allow trapped gas to be released into the production casing of a gas well (Economides et al., 1998). Water usage for hydraulic fracturing ranges from 3 - 7 million gallons for a single well in Marcellus (Gaudlip et al., 2008). About 10% - 30% of the injected fracturing fluid returns to the surface during the first 10-14 days, which is defined as flowback water (Kidder et al., 2011).

Flowback water contains chemicals that come from the fracturing fluid, such as diluted acids, biocides, viscosity modifiers, friction reducers and scale inhibitors, and those that come

from the formation water or dissolution of shale (GWPC and ALL, 2009). The flowback water is typically impounded at the surface for subsequent disposal, treatment, or reuse. Due to the large water volume, high concentration of dissolved solids, and complex physical-chemical composition of the flowback water, there is growing public concern about management of flowback water. These concerns result from the potential for human health and environmental impacts associated with release of untreated or inadequately treated flowback water to the environment (Kargbo et al., 2010). Flowback water management options in Marcellus Shale are confounded by high concentrations of total dissolved solids (TDS) and a lack of physical infrastructure for disposal in Class II underground injection control wells (Arthur et al., 2009; Kargbo et al., 2010). Hence, most of the flowback water in Marcellus Shale is reused for hydraulic fracturing of subsequent gas wells.

Acid mine drainage (AMD) is a potential water source that could alleviate low flowback water recovery by serving as a makeup water for the recycling and reuse of wastewaters in the Marcellus Shale development. AMD is particularly attractive water source due its proximity to natural gas well sites. In addition to serving as source water for hydraulic fracturing, AMD also provides source of sulfates (Akcil and Koldas, 2006) that can be used to precipitate Ba, Sr, and Ca in the flowback water and reduce the potential for scale formation in the gas well. Precipitates formed by the reaction of AMD with flowback water will have to be removed prior to water reuse to minimize the potential for porosity reduction of the proppant packing.

Membrane filtration was evaluated for the separation of solids formed after mixing representative AMD and flowback waters. This choice was based on a smaller footprint of membrane filtration compared to conventional granular media filtration and feasibility of use in field-deployable mobile treatment systems. Previous studies by Zhong et al. (2007) and AlZoubi

et al. (2010) focused on the use of reverse osmosis (RO) and nanofiltration (NF) membranes to remove dissolved constituents from AMD for final disposal. The objective of this study was to evaluate the potential of microfiltration to remove solids created after mixing AMD with flowback water with a particulate focus on the potential for membrane fouling. Barium sulfate and calcium carbonate are likely the major solids formed by the mixing of flowback water and AMD. Several studies showed the potential of barium sulfate scales to foul the reverse osmosis (RO) and hollow fiber membrane systems (Bonne et al., 2000).

This study was designed to evaluate the feasibility of membrane microfiltration to assist flowback recycling and reuse program in situation where AMD is used as a source of makeup water. Membrane filtration of actual flowback and AMD waters that were selected based on their proximity were performed in a dead-end bench-scale unit. Permeate flux analysis was accompanied by detail characterization of precipitates in terms of composition and particle size distribution to gain full insight into the potential for membrane fouling by this unique mixture.

2.0 LITERATURE REVIEW

2.1 FLOWBACK WATER

2.1.1 Flowback water disposal

Shale gas production always involves vertical and horizontal drilling, which require millions of gallons of water. During this process, a small portion of the injected water will return to the surface as flowback water. Sometimes, the flowback water will be treated on-site for further hydraulic fracturing. However, it is usually transported and disposed of in an impoundment or a pit for storage or further treatment. Normally, flowback water is not allowed to be discharged into surface waters before treatment, because it contains chemical additives from the fracturing fluids such as diluted acid, biocides, friction reducers and scale inhibitors. These chemical components may adversely impact the aquatic ecosystem and cause serious environmental pollution. More than that, the toxic chemicals present in the flowback water (Gaudlip et al., 2008) may kill or impact the animals or organisms in the water body. Also, the toxic heavy metals bio-accumulated in fish may potentially be transported up the food chain to cause serious health problems in human population. Therefore, the PADEP has recommended to public wastewater treatment plants not to accept flowback water to avoid further contamination of surface water and groundwater.

2.1.2 Flowback water disposal regulation

In the US, regulations and laws related to flowback water disposal are governed by the Underground Injection Control Program (UIC) of the Federal Safe Drinking Water Act, the Federal Clean Water Act and the National Pollutant Discharge Elimination System (NPDES). When involved in shale gas production, each state has its own concerns and risks of water resource impact. Therefore, each state usually has its own regulations to protect the environment while encouraging the development of shale gas resource (GWPC and ALL, 2009).

Pennsylvania established databases to monitor the quality of water resources strengthened the regulations relevant to flowback water disposal or treatment (PADEP, 2010). USEPA has begun a study to develop the regulations to guide discharges of wastewater from the Shale Gas Extraction (SGE) industry similar to effluent guidelines for 57 other industries that have been issued by USEPA and have effectively reduced the discharge of toxic pollutants into the environment (US EPA, 2011).

2.2 AMD POLLUTION AND REGULATIONS

Coal mine water normally contains high concentration of sulfates and metals, which have a great impact on the quality of receiving waters (river, lake, pond etc.). Sulfide oxidation in abandoned mine is a common phenomenon associated with the production of chemicals that can enter a water body, leading to a reduction in water quality through the increase of acidity, metals and dissolved salts. Therefore the Acid Mine Drainage (AMD) needs specific treatment before disposal due to its serious environmental impacts (Kleinmann, 1981; Nordstrom, 1982). The

treatment of AMD usually requires a pH adjustment and precipitation of heavy metals. The process involves addition of lime or other base followed by energy-intensive forced agitation and aeration processes (Cheng et al., 2011).

Mining operations are regulated under the Clean Water Act (CWA). The regulations relevant to AMD are mentioned in CWA Section 402. Part of the AMD generated from coal mining industries is regulated under the Surface Mining Control and Reclamation Act (SMCRA) of 1977. However, AMD treatment is not stringent in some states, which leads to the pollution of groundwater by the negligent and irresponsible management.

2.3 SUSTAINABLE METHODS TO TREAT FLOWBACK WATER

Application of hydraulic fracturing in shale gas drilling requires a considerable volume of water. The increasing consumption of groundwater or drinking water for hydraulic fracturing is of great concern to the public. The development of shale gas production related activities raise not only the use of water but also the potential impact on water resources (Rahm and Riha, 2012). Current water usage for gas production in Pennsylvania is relatively small when compared to power generation. Future development of shale gas industry will require more and more water withdrawal and it is necessary to figure out a sustainable method to improve the hydraulic fracturing process.

In this research, the treatment for the mixture of flowback water and AMD was studied. This approach aims to treat two sources of pollution at the same time and provide sufficient source water for subsequent hydraulic fracturing. The flowback from hydrofracturing includes inorganic salts, metals, and organics, which exhibit vastly different chemistry than the original

fracturing fluid. The AMD water can be used as a source of sulfate to precipitate Ba, Sr, and Ca salts. Subsequent treatment to remove major metal salts will produce fluids that are suitable for fracturing water reuse.

2.4 MEMBRANE FILTRATION

In recent years, membrane filtration shows an increasing effectiveness in surface water treatment when compared to conventional treatment technologies. However the fouling issue has always been a great concern for any field of application (Zularisam et al., 2006).

The total suspended solids created through the reaction between barium from flowback water and sulfate from AMD and calcium from flowback water and bicarbonate from AMD, range from 0.15 to 0.4 g/L depending on the waters tested. Membrane filtration is evaluated in this study for the removal of suspended solids. Suitability of membrane filtration depends not only on the removal efficiency but also on the permeate flux. Membrane fouling caused by the accumulation of suspended solids and macromolecules on the surface and inside the membrane pores is the main limitation to membrane filtration process. Generally, membrane fouling can be reduced by carefully selecting the membrane material and operating condition.

2.5 PROCESS PARAMETERS

Conventional notations for membrane filtration are described below and will be used throughout this document.

2.5.1 Permeate flux

The permeate flux is defined as the volume of permeate obtained per unit time and unit membrane area:

$$J = \frac{Q}{A} \quad (1)$$

where:

J = permeate flux ($\text{L h}^{-1} \text{m}^{-2}$)

Q = permeate flowrate (L h^{-1})

A = membrane surface area (m^2)

2.5.2 Permeability coefficient

The membrane permeability coefficient, commonly referred to as membrane permeability, is the permeate flux per unit of applied pressure:

$$L_p = \frac{J}{P} \quad (2)$$

where:

L_p = permeability coefficient ($\text{L h}^{-1} \text{m}^{-2} \text{bar}^{-1}$)

J = permeate flux ($\text{L h}^{-1} \text{m}^{-2}$)

P = applied pressure (bar)

2.5.3 Volume concentration factor

When the experiment is performed without permeate recycling, a volume concentration factor VCF (t) is defined as follow:

$$\text{VCF}(t) = \frac{V_f}{V_f - V_p(t)} \quad (3)$$

where:

VCF (t) = volume concentration factor as a function of time t

V_f = initial feed volume (L)

$V_p(t)$ = permeate volume (L) at the time t

2.6 FOULING MECHANISM THEORY

Experimental data can be used to better understand which of the four fouling mechanisms (Grace, 1956) control the permeate flux: 1) Cake filtration, 2) Intermediate blocking, 3) Standard blocking, and 4) Complete blocking. Duclos-Orsello et al. (2006) described the sequence of fouling mechanisms occurring during the filtration process, which was initially pore constriction (standard blocking) followed by pore blocking (complete blocking) and then cake filtration. Standard blocking is due to particles that are smaller than membrane pore size getting into the pores and constricting pore channels. Complete blocking is caused by the particles whose size is similar to the size of membrane pores block the entrance to pore channels. Once the membrane pores are blocked, particles will accumulate on the surface and form a cake layer, which further contributes to membrane fouling.

Hermia (1982) formulated the flux decline during filtration under constant pressure as follows:

$$\frac{d^2t}{dV^2} = k \left(\frac{dt}{dV} \right)^n \quad (4)$$

where:

t = time (s)

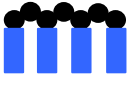



V = volume of permeate (L)

n = an exponent whose value characterizes the fouling mechanism (Table 1),

Grenier et al. (2008) simplified Equation (4) and applied it to characterize the fouling of various suspensions. The four corresponding linear equations related to the fouling mechanisms described above are presented in Table 1 and discussed below.

The fouling mechanism can be identified by plotting the filtration data using the corresponding linear form model. For example, to identify cake filtration, the filtration data should be converted to dt/dV and then plotted as a function of permeate volume (V). A linear relationship characterized by the linear regression factor can be used to evaluate how well the model fits the data and decide on the existence of a specific type of fouling in the filtration process.

Table 1. Fouling mechanisms and their corresponding physical basis (Grenier et. al., 2008)

Fouling mechanism	n	Corresponding linear form	Physical concept	
Cake filtration	0	$\frac{dt}{dV} = \frac{1}{Q} = f(V)$	Formation of a surface deposit	
Intermediate blocking	1	$\frac{dt}{dV} = \frac{1}{Q} = f(t)$	Pore blocking + surface deposit	
Standard blocking	1.5	$(\frac{dV}{dt})^{1/2} = Q^{1/2} = f(V)$	Pore constriction	
Complete blocking	2	$\frac{dV}{dt} = Q = f(V)$	Pore blocking	

3.0 MATERIALS AND METHODS

3.1 FEED WATER

3.1.1 Feed water collection and preparation

Samples of Marcellus Shale flowback waters were collected from two separate well sites (site A and B) located in southwest Pennsylvania over a period of days. The flow composite water sample for each site was prepared by mixing daily water samples in proportion to the flow rate that was recorded at the time of sample collection. The water sample collection and preparation of the flow composite sample are described below.

The site A in Westmoreland County (East of Allegheny) had only one well on the pad. The site B in Washington County (South West of Allegheny) had five wells that were connected in a common manifold. The volume of fracturing fluid injected for the hydraulic fracturing was 4.33 million gallons for the single well at site A and 18 million gallons for the five wells at site B (which corresponds to an average of 3.6 million gallons per well). Flowrate profiles were similar for the two sites (Figure 1 and Figure 2). A sharp decrease occurred during the first four days and the flowrate stabilized at a low value after the fifth day. The fluctuation of the flowrate for the site A was mainly due to well maintenance (pipe changes).

The water recovery varied depending on the site but remained low. After 15 days, only 7% of the injected volume was recovered at site A. The site B showed slightly higher water recovery of 14.5% after 20 days. These results confirmed the fact that the majority of the fracturing fluid remained in the formation. The fluid would continue to flow back but at a flowrate of 400 to 1700 gallons per day during the lifetime of the well. In sum, the water recovery rates were 10% and 15% of the total fracturing fluid for site A and site B, respectively.

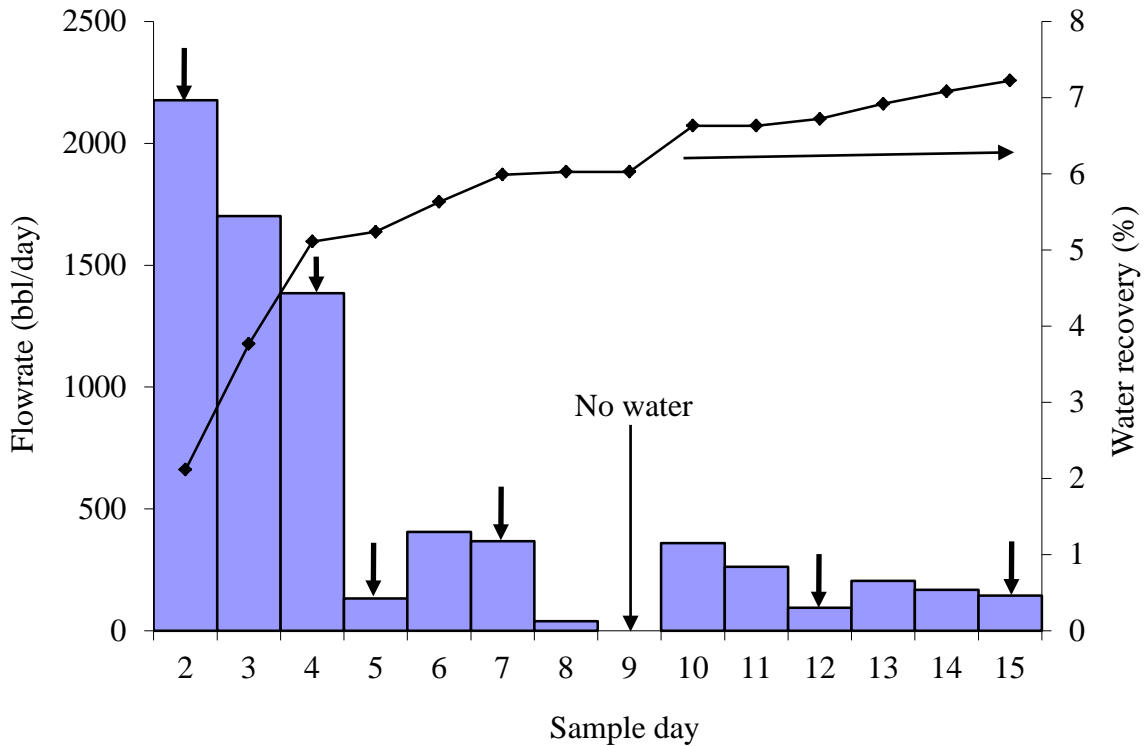


Figure 1. Flowback water flowrate and water recovery for the site A (arrows mark days when the samples were collected)

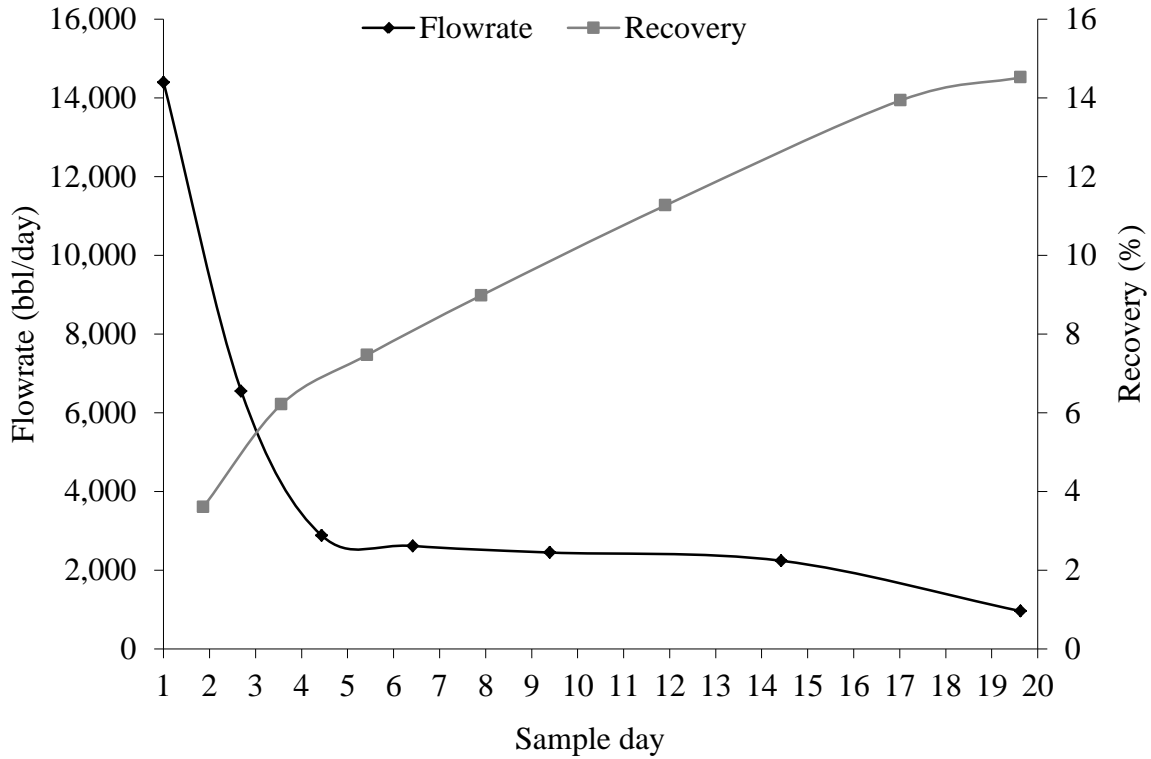


Figure 2. Flowback water flowrate and water recovery for the site B

The fracture of the flowback water recovered at each site at the time of sampling is summarized in Table 2. For Flowback water A, six samples were collected on day 1+2, 4, 5, 7, 12, 15. For Flowback water B, seven samples were collected on day 1, 3, 5, 7, 10, 15 and 20. All samples were individually stored in clean buckets and covered with lids. The composite flowback water samples were prepared based on the percentage of volume recovered for each individual sample. When preparing the flowback composite samples, samples from the buckets were taken offer each bucket was fully mixed with a mechanical mixer. These samples were placed in 2L volumetric flask and were mixed by inverting the flask several times. To avoid bacteria growth, the composite samples were stored in a refrigerator prior to use.

Table 2. Composition of the flowback water composite: Flowback water A and Flowback water B

Flowback water A		Flowback water B	
Sample day	Volume percentage	Sample day	Volume percentage
1+2	40.7%	1	24.8%
4	30.1%	3	18%
5	4.5%	5	8.6%
7	12.1%	7	10.4%
12	8.2%	10	15.8%
15	4.4%	15	18.4%
-	-	20	4%

The composite samples of Flowback water A and B were analyzed for total suspended solids (TSS), total dissolved solids (TDS), pH, alkalinity and major ions. Major cations were measured using atomic absorption spectrometry (GBC908, GBC Scientific Equipment LLC, Hampshire, IL and Perkin-Elmer model 1000) with air-acetylene or nitrous oxide-acetylene flame. All samples were filtered through a 0.45 μm filter before measurement. Major anions were analyzed by Dionex DX-500 ion chromatography system with IonPac® AS14A column at the carrier flow rate of 1mL/min. Alkalinity was measured using the standard method 2320B. TDS and TSS measurements were performed according to with standard methods 2540C and 2540D, respectively. pH was measured with a digital meter (Accument XL60, Fisher Scientific). Water characteristics for each composite flowback water sample are listed in Table 3.

AMD samples were collected from discharges located in the vicinity of each gas wells. They would serve as logical choices for makeup water for hydraulic fracturing operations in that area. Each AMD location was within 10 miles of the corresponding gas well. AMD 1 represents untreated discharge in the vicinity of Flowback Water A. AMD 2 represents a discharge in the vicinity of Flowback Water B that was treated in a passive water treatment system comprised of

lime addition followed by aeration and sedimentation. Water quality characteristics of the two AMD samples are listed in Table 3. All major ions, TSS, TDS, pH and alkalinity of AMDs were measured using the same methods as for the flowback waters.

As can be seen in Table 3, barium was found in both Flowback water A and B, but not in AMD 1 and 2. High TDS was found in both Flowback water A and B, which is common in general flowback waters (Kargbo et al., 2010). Table 3 shows a significant difference between Flowback water A and Flowback water B regarding ion concentration, TSS, TDS, turbidity and TOC. Sulfate in AMD 1 was much higher than in AMD 2 while iron in AMD 2 was negligible due to passive treatment of AMD 2. Higher concentration of both barium and sulfate in Flowback water A and AMD 1, respectively, indicate more barium sulfate would be precipitated when these waters are mixed then when Flowback water A is mixed with AMD 2. Higher concentrations of calcium and alkalinity in Flowback water B and AMD 2, respectively, indicate that more calcium carbonate with precipitate when these waters are mixed then when Flowback water A is mixed with AMD 1. These differences are critical for understanding the impact of flowback water and AMD compositions on the performance of membrane filtration processes.

Table 3. Flowback and AMD water characteristics

	Flowback water A	AMD 1	Flowback water B	AMD 2
Na (mg/L)	11860	104.1	27946	687.31
Ca (mg/L)	2170	76.2	15021	244.65
Mg (mg/L)	249	49.1	1720	33.25
Fe (total) (mg/L)	-	32.1	-	ND
Ba (mg/L)	730.5	ND	236	ND
Sr (mg/L)	362	1.5	1799	3
Cl (mg/L)	29000	70.8	104300	373.4
SO ₄ ²⁻ (mg/L)	-	708.7	14.8	242.5
TSS (mg/L)	98 (312 [*])	118	776 (593 [*])	1
TDS (mg/L)	38000 (37000 [*])	1328	166484 (148400 [*])	1574
Turbidity (NTU)	60	7.4	18	0.5
TOC (mg/L)	52	-	132.7	-
Alkalinity (mg CaCO ₃ /L)	-	40.5	44	393.8
pH	7.42	6.14	6.40	7.03

^{*} The TSS and TDS determined after filtration through 0.05 µm membrane.

3.1.2 Feed water

Two sets of water samples for membrane filtration experiments were prepared in this study based on the water recovery for each gas well. Mixture 1 was comprised of 10% Flowback water A and 90% AMD 1 while Mixture 2 was comprised of 15% Flowback water B and 85% AMD 2. Each water sample was allowed to equilibrate for at least 12 hours before the filtration experiments to ensure chemical equilibrium during the filtration test.

Filtration tests for each set of samples were conducted using three different feed water samples to gain insight into microfiltration process and potential fouling mechanisms: 1) a mixture of flowback water and the corresponding AMD, 2) AMD alone, and 3) flowback water alone. Filtration experiments with only AMD or flowback water samples were conducted after dilution with distilled water at the same ratio that was used in preparing the mixture of the two to maintain similar composition of original water constituents in all cases. The volume of each feed solution was 2 L.

3.2 PARTICLE SIZE DISTRIBUTION

Particle size distribution in each feed mixture was determined using Microtrac S3500 Particle Analyzer (Microtrac, York, PA; Measurement basic range (wet): 0.7 μm – 1000 μm). Size distribution for particles in the sub-micron range was determined using a Zetasizer Nano S (Malvern, Worcestershire, UK; Measurement range: 0.3nm – 10.0 μm).

3.3 TOC

The total organic carbon (TOC) in water samples was analyzed using 1010 Total Organic Carbon Analyzer equipped with a 1051 Vial Autosampler (American Laboratory Trading, East Lyme, CT).

3.4 DEAD-END MEMBRANE FILTRATION

Membrane filtration experiments were conducted using a magnetically stirred dead-end cell with 340 mL volume (Figure 3) operated in a constant pressure mode. A 2.5 L feed tank was connected to the dead-end cell and was pressurized using a compressed nitrogen tank to allow filtration of a larger suspension volume. The membrane filtration experiments were conducted using hydrophilic PVDF 0.22 μm microfiltration membranes (Durapore[®] Millipore, Billerica, MA). The membrane was cut into a circle with a diameter of 7.5 cm and was supported by a porous metal plate located at the bottom of the dead-end cell. Permeate was collected and weighed throughout the filtration test. All experiments were performed at room temperature (20 - 22°C) with a constant pressure of 0.5 bar (7.2 psi). New membrane was used for each filtration experiment. The initial membrane permeability with deionized water of approximately $5800 \text{ L h}^{-1} \text{ m}^{-2} \text{ bar}^{-1}$ was verified before each test.

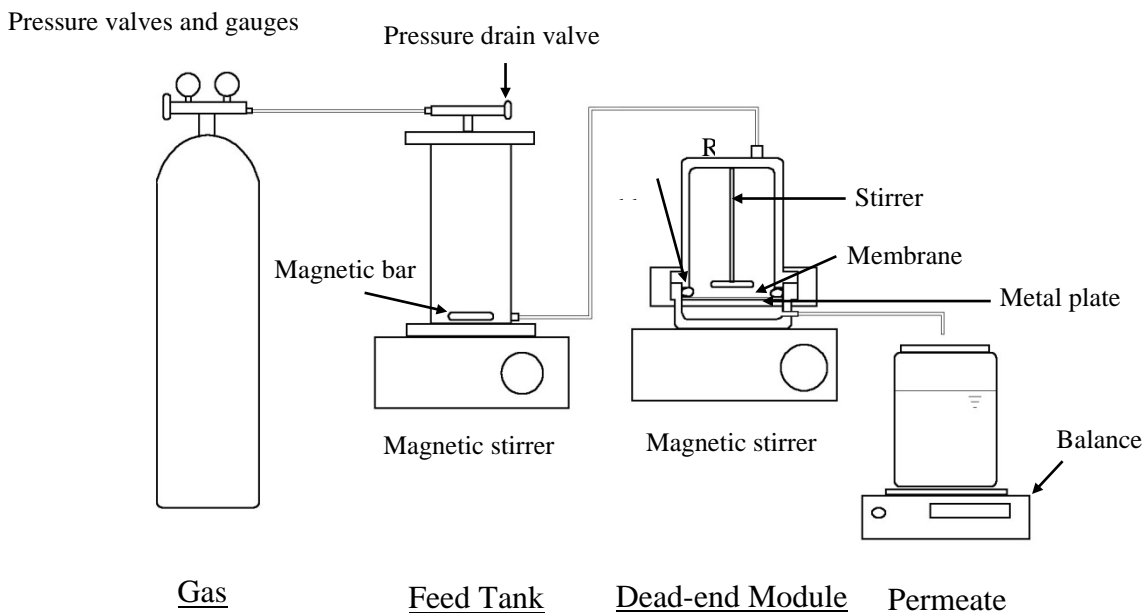


Figure 3. Experimental dead-end membrane filtration apparatus

3.5 COAGULATION AND FLOCCULATION

The coagulation and flocculation experiments with Mixtures 1 and 2 were performed using a PB-700 Six Paddle Jar Tester (Phipps & Bird, Richmond, VA). The total organic carbon (TOC) and turbidity of two feed waters were measured before and after coagulation - flocculation processes. Each beaker was filled with 500 mL of feed water for coagulation process. Coagulant stock solutions were prepared in a 1L volumetric flask before each round of experiments and were stored in clean plastic bottles. The pH was adjusted during the rapid mixing process using 0.1 M HCl or NaOH. All equipments and glass beakers were cleaned for each experiment. All tests were conducted at room temperature (~20°C).

G (s^{-1}) is the velocity gradient and Gt (where t (s) is the detention time) is a unitless parameter, normally used to quantify the mixing intensity. In the coagulation/flocculation process used in water and wastewater treatment, a Gt value of around 10,000 is typically used (Viessman and Hammer, 1985). The rating curve of velocity gradient (G , s^{-1}) versus agitator paddle speed in units of round per minute (rpm) for a 2-liter beaker was provided by Phipps & Bird. This curve was used to calculate the G values for the 0.5-liter jar test by converting the G value as function of volume (V , m^3) based on the velocity gradient equation:

$$G = \sqrt{\frac{P}{\mu V}} \quad (5)$$

where:

G = velocity gradient (sec^{-1})

P = global power input ($N \cdot ms^{-1}$)

μ = dynamic viscosity of water sample ($0.001 N \cdot sm^{-2}$).

V = volume of water sample (m^3)

Since the power input for the jar test device remains the same, the converting equation for G values is:

$$\frac{G_0}{G_n} = \sqrt{\frac{V_n}{V_0}} \quad (6)$$

where:

G_0 = velocity gradient (sec^{-1}) for 2-liter beaker jar test

G_n = velocity gradient (sec^{-1}) for n-liter beaker jar test

V = volume of water sample (m^3) for 2-liter beaker jar test

V = volume of water sample (m^3) n-liter beaker jar test

For the coagulation process, rapid mixing was conducted for 2 minutes at the speed of 300 rpm ($G = 760 \text{ sec}^{-1}$) followed by slow mixing for 15 minutes at the speed of 25 rpm (velocity gradient, $G = 36 \text{ sec}^{-1}$) and 40 minutes of settling. After 40 minutes of settling, two 100 mL samples from each jar were taken at a depth of 100 mm in the beaker for turbidity and TOC measurements. The Gt values for coagulation and flocculation process were 91200 and 32400, respectively. The high Gt value in rapid mix process was inevitable because the time spend on pH adjustment was at least 1.5 minutes.

Two coagulants were selected for the coagulation- flocculation experiments: Aluminium Chloride ($\text{AlCl}_3 \cdot 6\text{H}_2\text{O}$) and Ferric Chloride ($\text{FeCl}_3 \cdot 6\text{H}_2\text{O}$). The efficiency of coagulation - flocculation process was evaluated by the comparison of turbidity and TOC removal. For each coagulant, the initial dosage and pH were tested under conditions listed in Table 4.

Table 4. Coagulant dose and pH conditions tested

Aluminium Chloride	
Initial added dose as Al (mg/L)	10, 20, 30, 40, 50, 60
pH	3, 4, 5, 6
Ferric Chloride	
Initial added dose as Fe (mg/L)	10, 20, 30, 40, 50, 60
pH	3, 4, 5, 6

4.0 RESULTS AND DISCUSSION

4.1 MEMBRANE FILTRATION

4.1.1 Particle size distribution

The raw flowback waters were analyzed by light scattering (Microtrac S3500) in micrometer range to determine their particle size distribution. A 100mL test sample for each round of analysis was prepared and stored in a clean bottle. The only the sample of Flowback water A was filtered through 0.45 μ m glass fiber membrane before particle size distribution analysis because the high turbidity in Flowback water A would interfere with the accuracy of results.

As shown in Figure 4, the result indicated that the majority of particles in Flowback water A were in size of 3.1 μ m. The results for Flowback water B depicted on Figure 5 indicate that the majority of particles were in size is 8.1 μ m. For both Flowback water A and B, no particles smaller than 1 μ m were detected by Microtrac S3500.

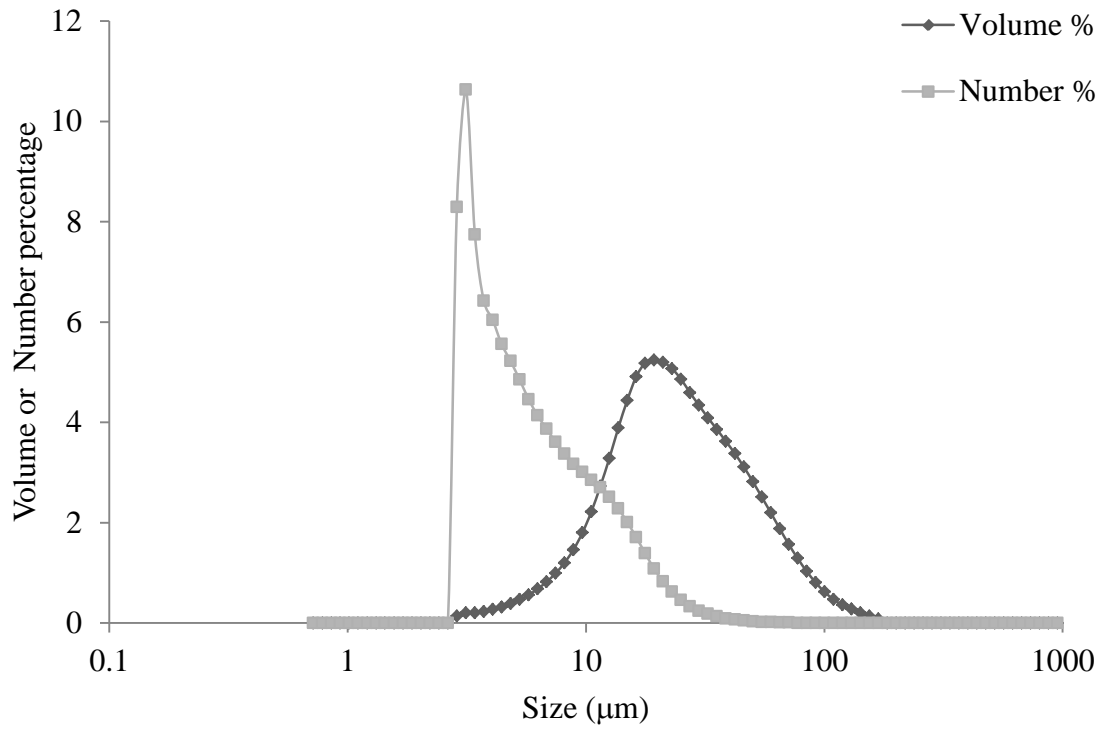


Figure 4. Particle size distribution measured using Microtrac S3500: Flowback water A

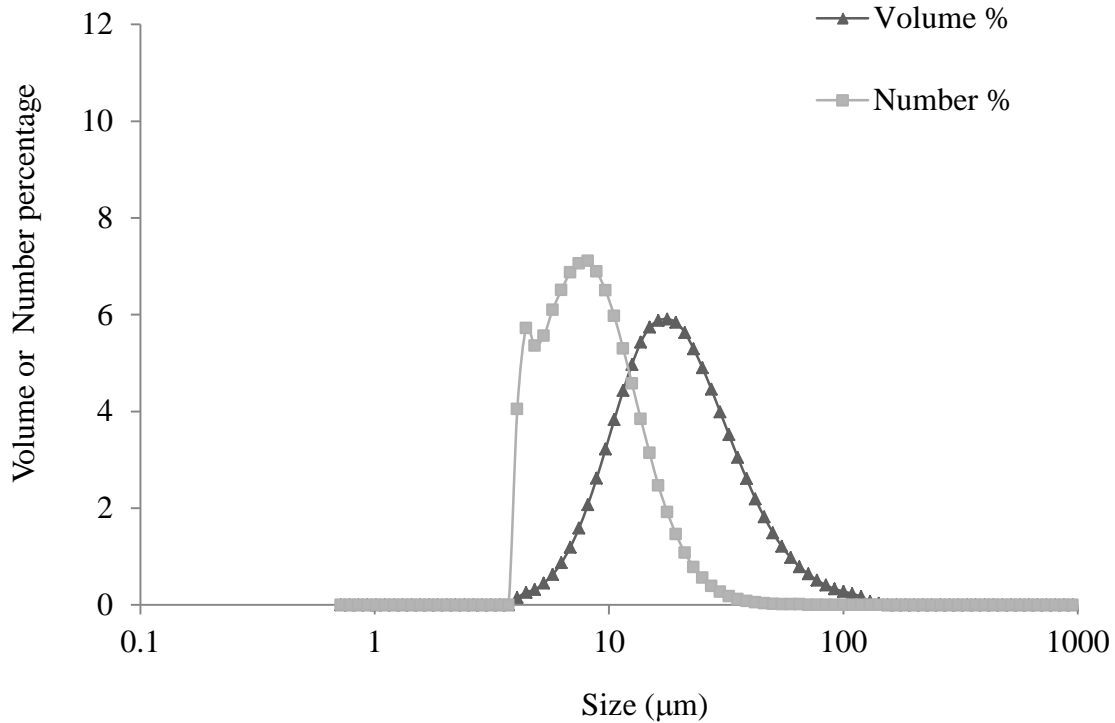


Figure 5. Particle size distribution measured using Microtrac S3500: Flowback water B

Figure 6 and 7 depict the particle size distribution results for the two mixtures. These results suggested that the particles size in Mixture 1 decreased compared to Flowback water A, while the impact of AMD 2 addition to Flowback water B was negligible in terms of the resulting particle size distribution. The particles size decrease after adding AMD 1 into Flowback water A may be due to the generation of barium sulfate, which typically has a size range of 1 – 4 µm. On the other hand, calcium carbonate that forms after mixing Flowback water B and AMD 2 has particles size of about 10 µm, which resulted in a minimal impact on particle size distribution of Flowback water B. Figure 6 shows that the particle size in the Mixture 1 ranged from 1 to 65 µm with the majority of the particles between 1 and 10 µm. Figure 7 shows that the particle size in Mixture 2 ranged from 4 to 120 µm with the majority of particles between 4 and 20 µm.

Based on the results of particle size distribution generated by Microtrac S3500, it was expected that a microfiltration membrane with a pore size of 0.22 μm would be efficient for removing these particles from the solution, since its pore size was an order of magnitude lower than the crystal size.

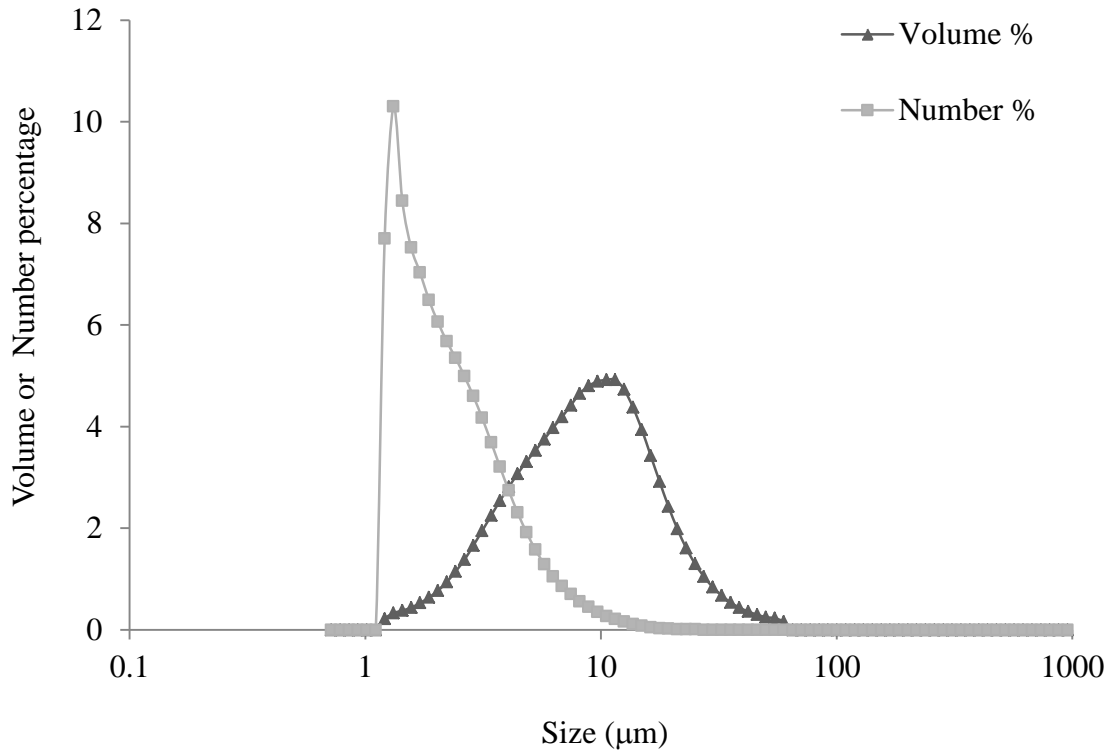


Figure 6. Particle size distribution measured using Microtrac S3500: Mixture 1

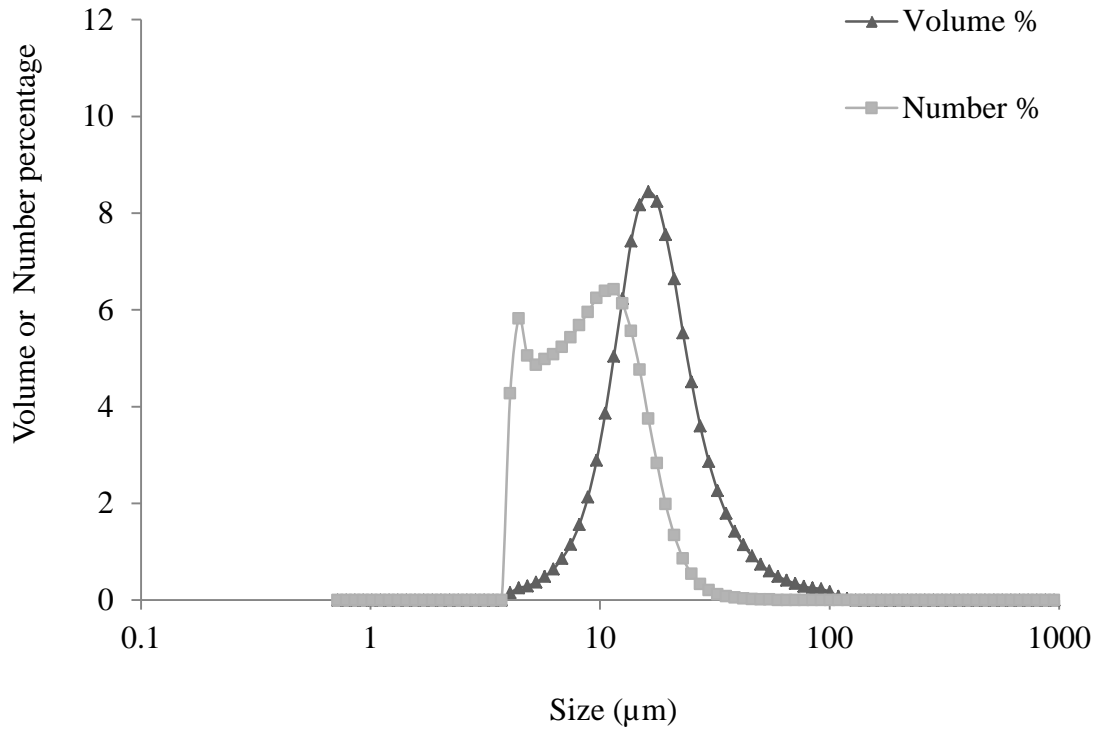


Figure 7. Particle size distribution measured using Microtrac S3500: Mixture 2

4.1.2 Permeate flux behavior

In the filtration experiment with Mixture 1, the flux dramatically declined during the first 8 minutes (Figure 8)). A severe fouling occurred immediately after the filtration started and the initial permeate flux was about 70% of the clean water flux. The flux behavior during the membrane filtration of Mixture 2 revealed that the initial permeate flux was 98% of the clean water flux and the flux declined slowly and regularly. In contrary to the filtration of Mixture 1, no severe fouling was observed in the case of Mixture 2.

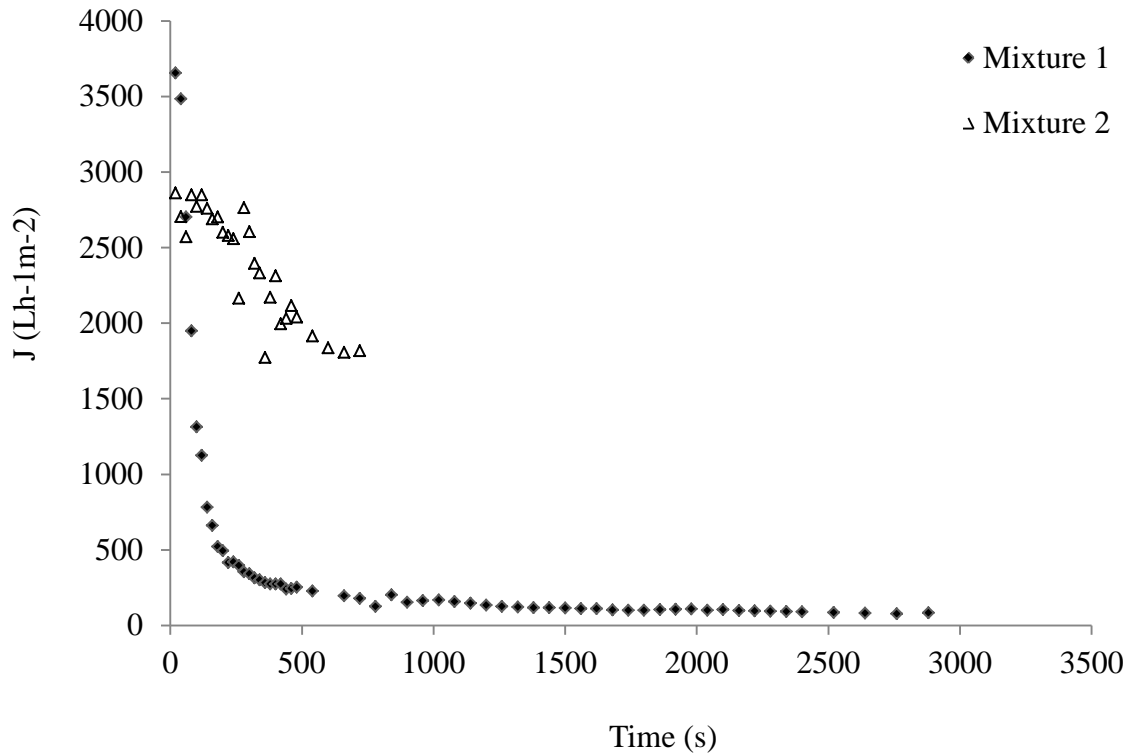


Figure 8. Permeate flux vs. time for Mixture 1 and Mixture 2

Possible foulants in the mixture of flowback water and AMD are the barium sulfate crystals, the iron oxide, the organic matter present in the flowback water, and the total suspended solids from the flowback water. Therefore, further filtration experiments were conducted with components of these mixtures to identify the causes of membrane fouling. The flowback water and AMD were diluted with DI water at the same ratio used in the Mixture.

Volume concentration factor (VCF) was used instead of time for plotting the permeate flux data, which was a commonly used method to unify the x axis from experiments with different total filtration times. The permeate flux decline with VCF for the three filtration experiments of Mixture 1 and 2 is plotted on Figure 9 and 10, respectively.

In Figure 9, the permeate flux decreased much slower when AMD 1 is filtered compared with the diluted Flowback water A and the Mixture 1. In addition, Figure 9 shows the permeate flux for diluted Flowback A and Mixture 1 had identical behavior of a fast flux decline during the first few minutes of filtration. Figure 10 indicates that AMD 2, Flowback water B and Mixture 2 had similar slowly declining flux and that there was no severe fouling of the membrane like in the case of Flowback water A and Mixture 1. The permeate flux for diluted Flowback water B and Mixture 2 showed identical behavior of a slow flux decline during the filtration process. These behaviors clearly demonstrate that the addition of AMD into flowback water had negligible effect on permeate flux behavior. Furthermore, the filtration behavior of Flowback water A and B (Figure 11) indicates that the foulants responsible for the severe membrane fouling are components that are present in Flowback water A.

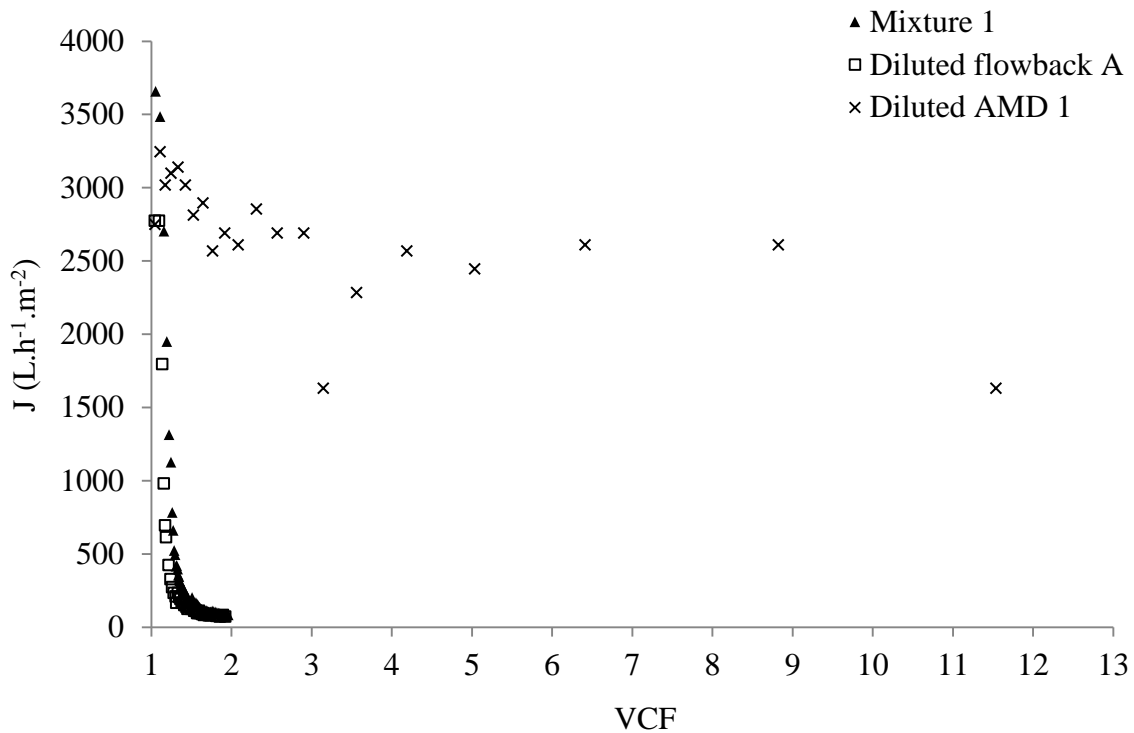


Figure 9. Permeate flux vs. VCF for Mixture 1, diluted Flowback water A and diluted AMD 1

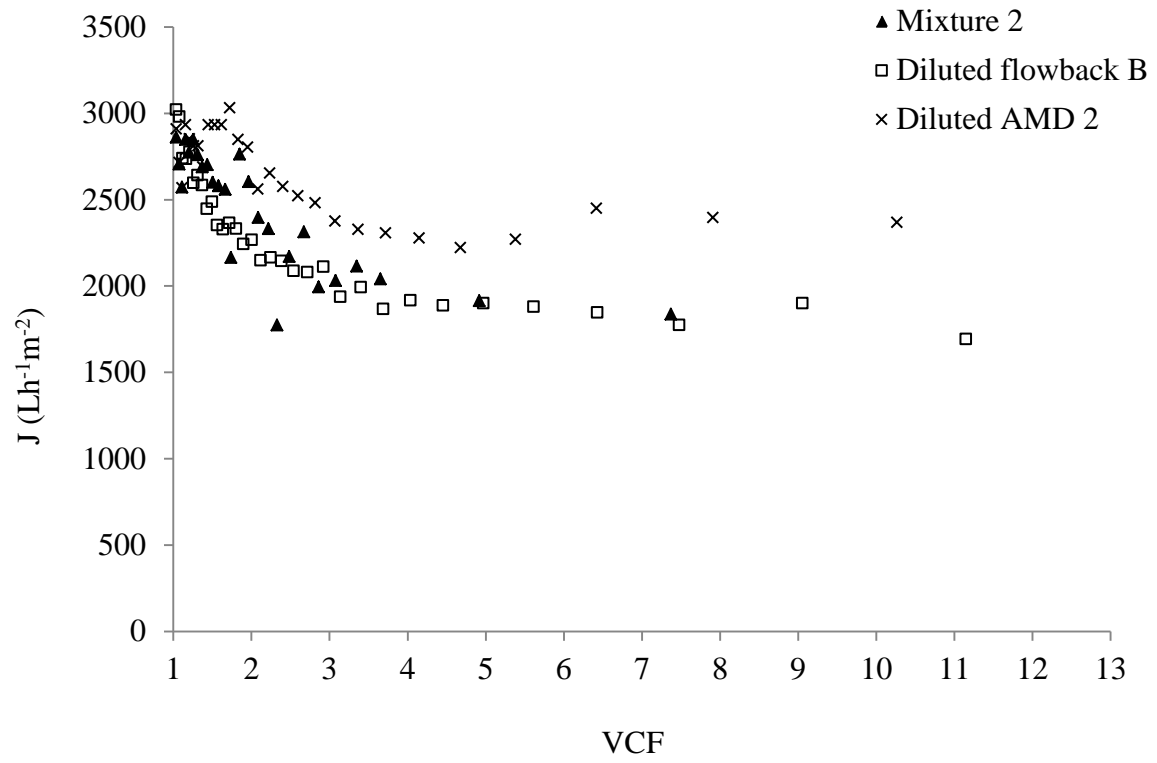


Figure 10. Permeate flux vs. VCF for Mixture 2, diluted Flowback water B and diluted AMD 2

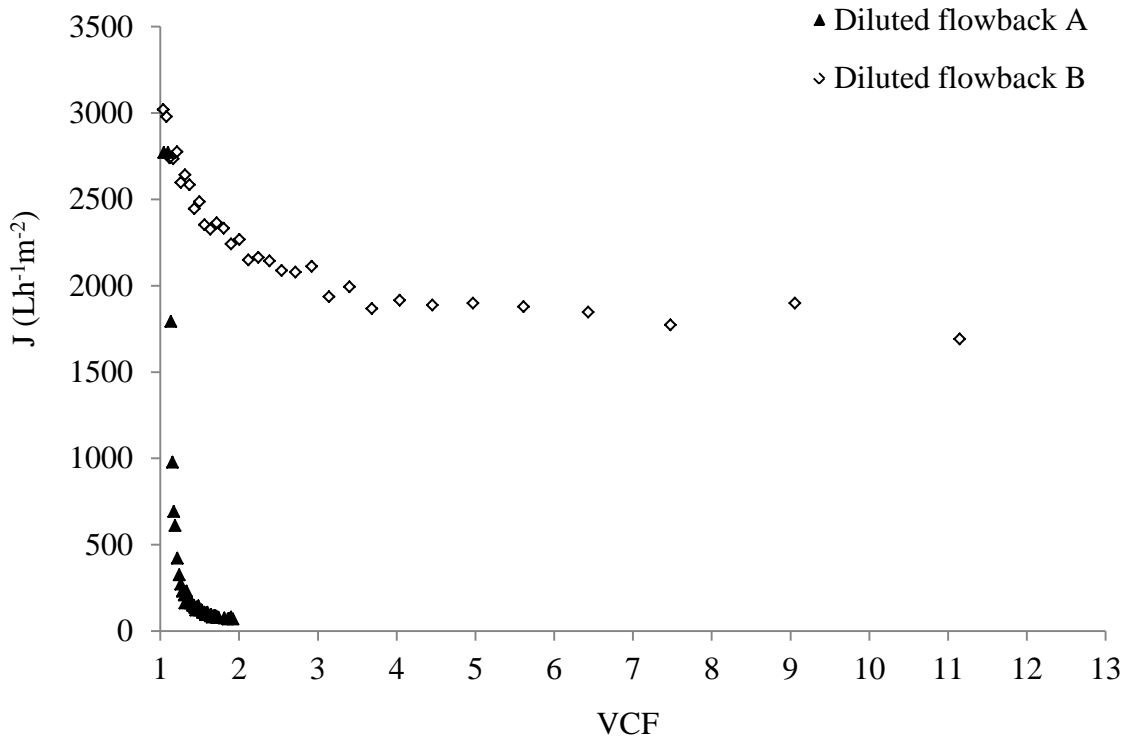


Figure 11. Permeate flux vs. VCF for diluted Flowback water A and Flowback water B

The AMD by itself caused fairly low permeate flux decline, which was indicated by much higher steady state flux of AMD 1 compared to that of diluted Flowback water A and Mixture 1 (Figure 9). The permeate flux of the AMD 1 decreased and stabilized at 2500 L h⁻¹ m⁻² at a VCF of 3 and showed no dramatic flux decline during the filtration process. For diluted AMD 2, the permeate flux was slightly higher than for the diluted Flowback water B and the Mixture 2 (Figure 10). When comparing the filtration tests with AMD 1 and AMD 2, identical flux behavior was observed (Figure 12). This further confirmed that AMD has negligible impact on membrane fouling.

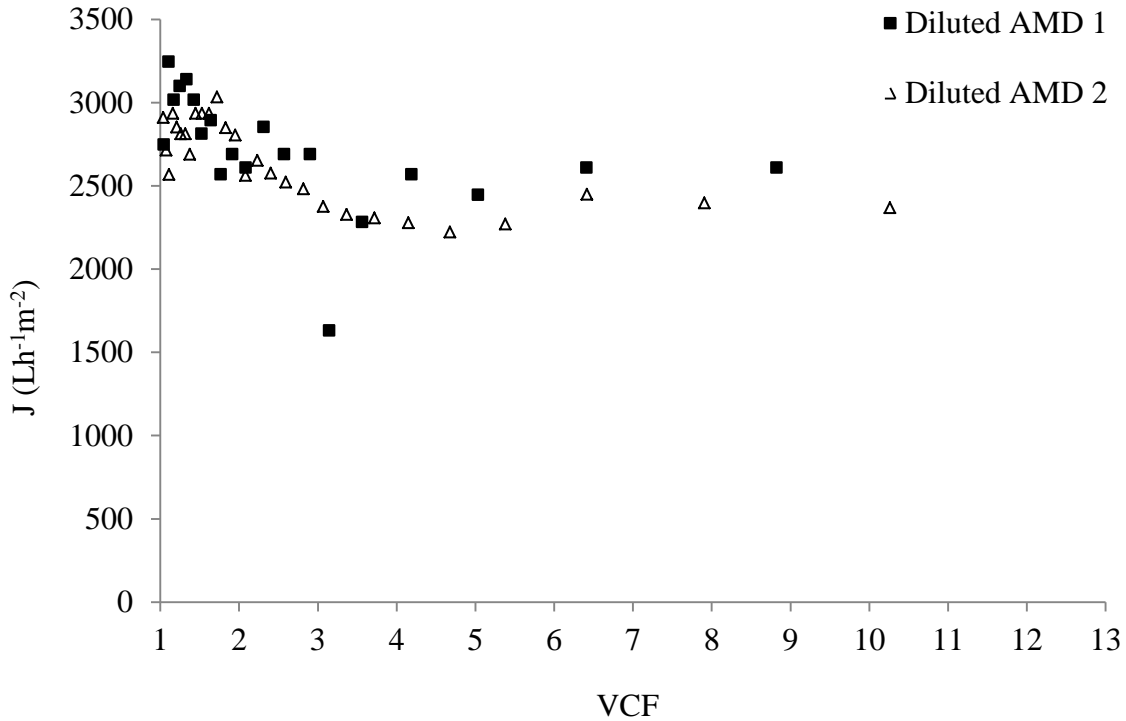


Figure 12. Permeate flux vs. VCF for diluted AMD 1 and diluted AMD 2

As discussed, the components in AMD caused negligible fouling compared to what was contained in the flowback water. However, barium sulfate crystals in the mixtures could be a reason for membrane fouling.

Barium sulfate fouling was observed in membrane filtration processes, such as the reverse osmosis (RO) (Bonne et al., 2000). However it is unclear whether it adversely deteriorated the microfiltration performance in this study. Therefore, filtration experiments with barium and sulfate solutions were conducted to investigate the impact of barium sulfate on membrane fouling during the microfiltration process. Since no severe fouling occurred during the filtration of Mixture 2 or Flowback water B or AMD 2, the AMD 2 was used as the sulfate

source to generate $\text{BaSO}_4(\text{s})$ that would be subjected to microfiltration. In this case, any fouling of the microfiltration membrane would clearly result from the barium sulfate.

A comparison of membrane filtration was performed with two sets of water samples: 1) Sample 1: mixture of 1.7 L AMD 2 and 0.3 L Barium solution (barium concentration is 236 mg/L), 2) Sample 2: mixture of 1.7 L AMD 2 and 0.3 L Barium solution (barium concentration is 1964 mg/L). All barium solutions were prepared by dissolving $\text{BaCl}_2 \cdot 2\text{H}_2\text{O}$ (Barium Chloride, Dihydrate, Assay 99.0%, Mallinckrodt Chemicals) in deionized water. Before membrane filtration, each sample was mixed at least 12 hours to reach chemical equilibrium for barium sulfate precipitation. The concentrations of barium sulfate generated after the mixing process of two samples are summarized in Table 5.

Table 5. Barium sulfate concentration in Sample 1 and 2

	$\text{BaSO}_4 (\text{s})$ (mg/L)
Sample 1	86
Sample 2	501

As shown in Figure 13, the permeate flux slightly declined for both samples. Although the concentration of barium sulfate that precipitated in Sample 2 was six times as large as that in Sample 1, Figure 13 shows identical permeate flux decline for both samples. Therefore, the barium sulfate that precipitated during the mixing of flowback water and AMD had no impact on membrane filtration.

In conclusion, the barium sulfate created by the reaction of the flowback water and AMD has no impact on membrane filtration process. The main reason for severe fouling in the

filtration of Mixture 1 and Flowback water A was due to specific characteristics of the Flowback water A.

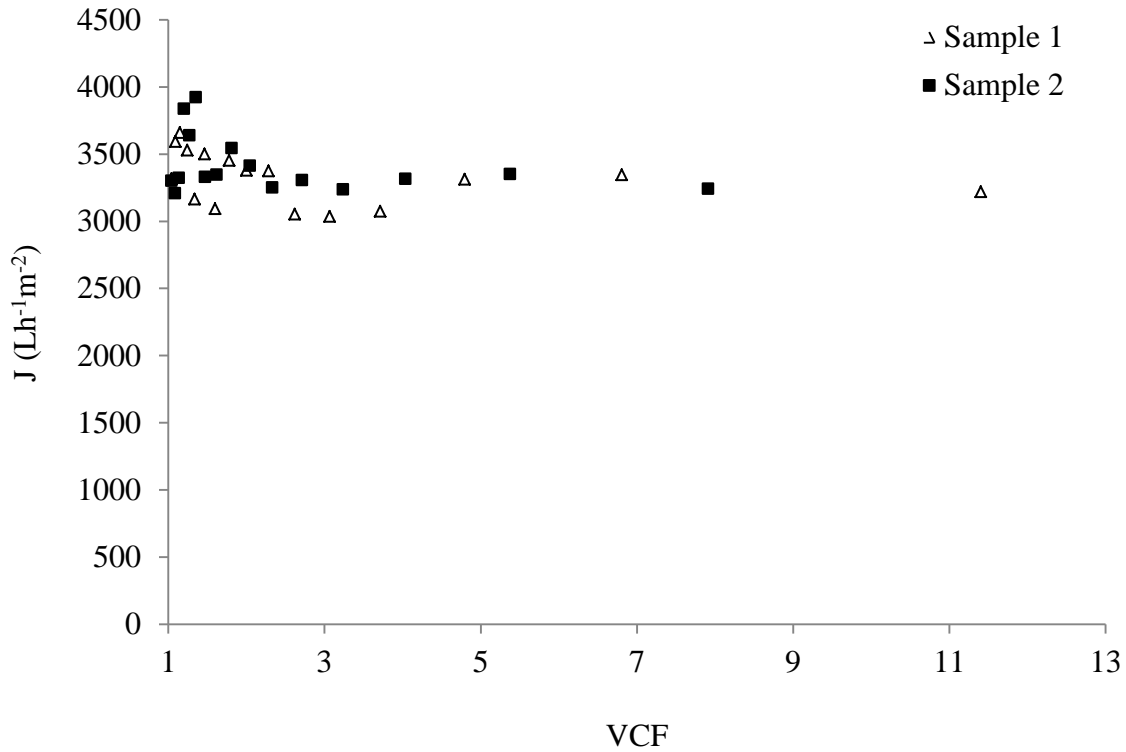


Figure 13. Permeate flux vs. VCF for Sample 1 and Sample 2

4.1.3 Fouling mechanism identification

Grenier et al.'s (2008) fouling mechanism models were applied to determine the type of fouling in each filtration experiment. Fouling mechanisms were identified by analyzing permeate flux data to better understand the membrane fouling phenomena. In this study, the fouling mechanism models were used to find out what caused the fouling and how the fouling formed during the membrane filtration.

The results of fouling mechanism analysis for Mixture 1 are included in Figures 14 to 18. In the early stages of filtration, standard blocking and complete blocking are indicated by the linear relationship of data shown in Figure 14 and 15, respectively. In the case of Mixture 1, particles detected by Microtrac S3500 had an average size of 1.3 μm , which was larger than the membrane pore size of 0.22 μm and should not be able to cause the pore constriction or even pore blocking. Figures 14 and 15 suggest that there are some particles in a sub-micron range in Mixture 1 or flowback A that were not detected by Microtrac S3500. In addition, these two fouling mechanisms cannot be fully characterized due to the high fouling speed and limited amount of data in that phase of the experiment. Therefore, to further understand the fouling mechanisms in the early stages of filtration, sub-micron particle size distribution of Flowback water A was performed on the filtrate that passed through 0.45 μm membrane.

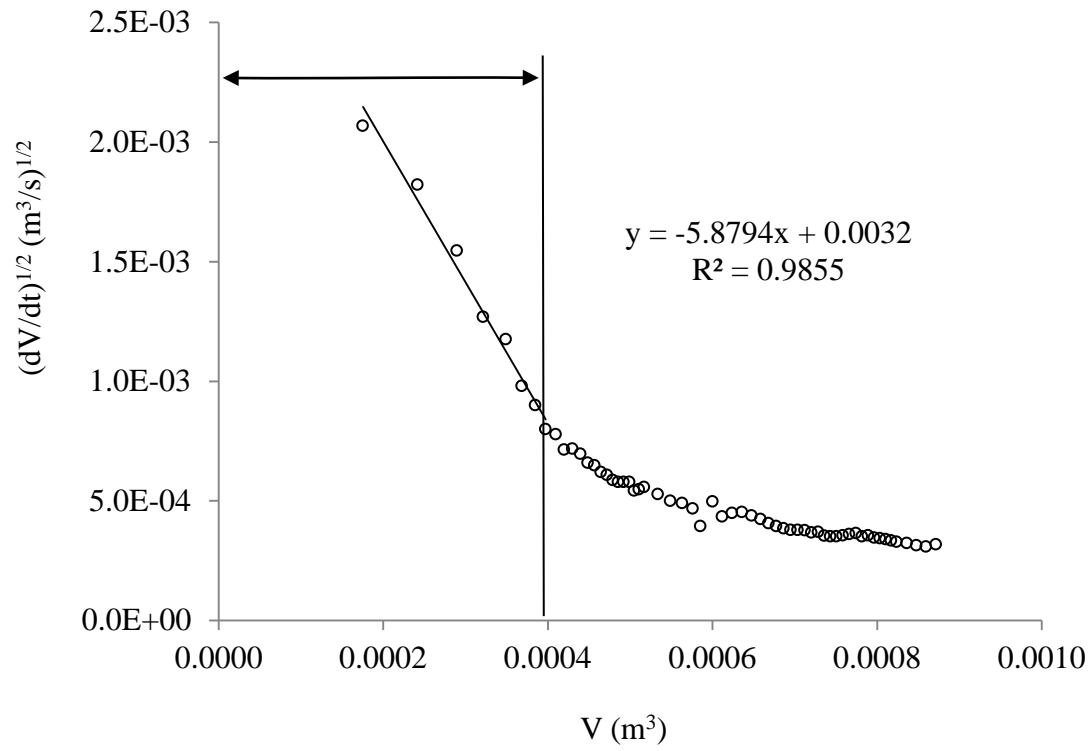


Figure 14. Fouling mechanism identification for the Mixture 1: Standard blocking

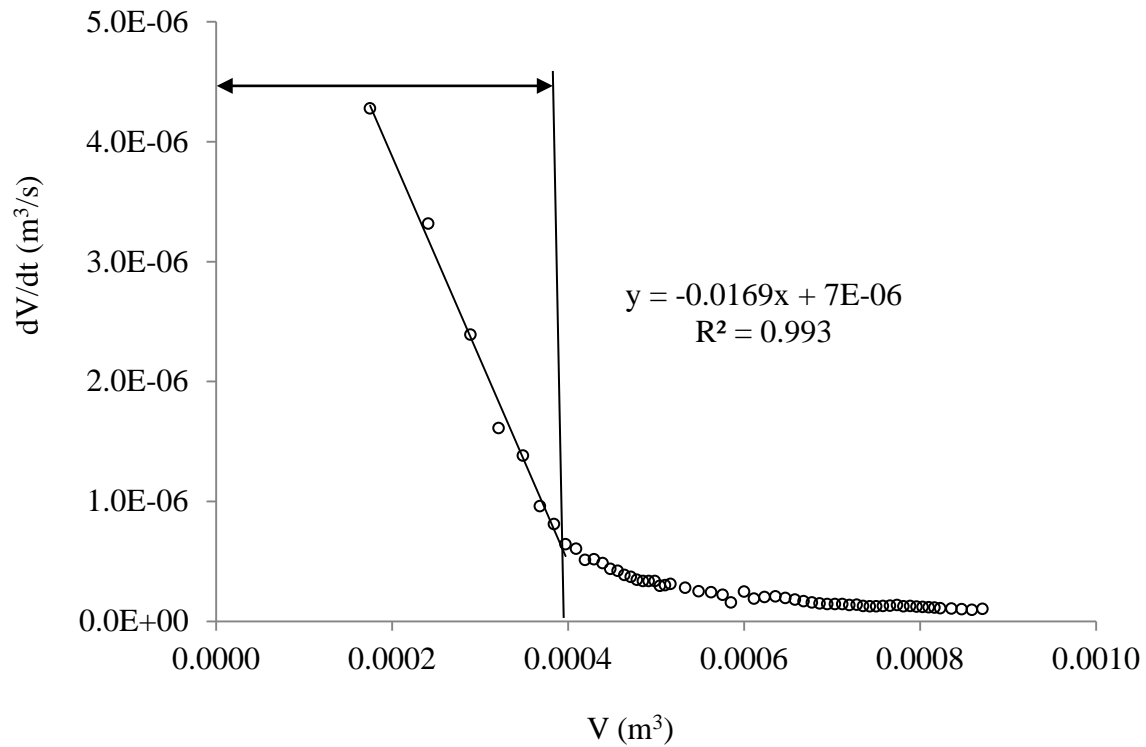


Figure 15. Fouling mechanism identification for the Mixture 1: Complete blocking

Zetasizer Nano (Malvern) was used to detect particles in the sub-micron range. In order to detect the smaller particles existing in Flowback water A without the interference of bigger particles, 100 mL solution was prepared by filtering Flowback water A through a 0.45 μm glass fiber filter, and analyzed by Zetasizer Nano (Malvern). The particle size distribution shown in Figure 16 revealed a peak at 0.11 μm . Particles in this size range are smaller than the membrane pore size of 0.22 μm and could go into the membrane to constrict the pore channel or cause a complete blocking of membrane pore. These results clearly support the physical concept that particles with size in the range of the microfiltration membrane pore diameter are able to induce pore blocking and pore constriction. Zetasizer Nano (Malvern) was used to analyze the particle size distribution for Flowback water B as well. The sample was filtered through a 0.45 μm glass

fiber filter before particle size analysis. No reliable (scatter) results of particles in sub-micron range were found, which may due to the interference caused by bigger particles in Flowback water B.

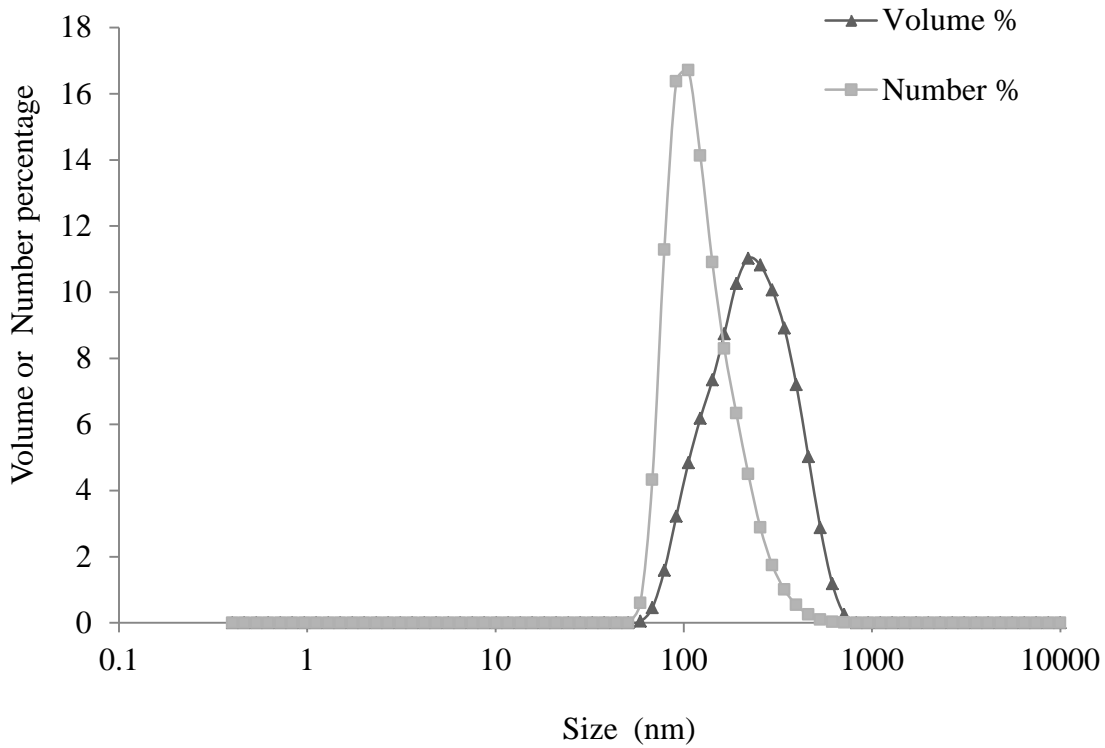


Figure 16. Particle size distribution measured using Malvern Zetasizer: Flowback water A

In the later stages of filtration experiments with Mixture 1, cake filtration and intermediate blocking were the main fouling mechanisms as shown in Figure 17 and 18, respectively. Linear relationship, which indicates cake filtration, was observed in Figure 17 where dt/dV was plotted as a function of permeate volume (V). When comparing the regression fits in Figures 17 and 18, membrane fouling due to cake filtration offered a better fit for the fouling model. Thus, for the complete filtration process of Mixture 1, the cake filtration was the

dominant fouling mechanism after standard blocking and complete blocking occurred during the early stages of the test. In conclusion, standard blocking and complete blocking caused by the particles in the sub-micron range were the dominant fouling mechanisms during the first few minutes of filtration based on the rapid flux decline. After that, cake filtration and intermediate blocking occurred by a formation of a cake deposit on the surface of membrane.

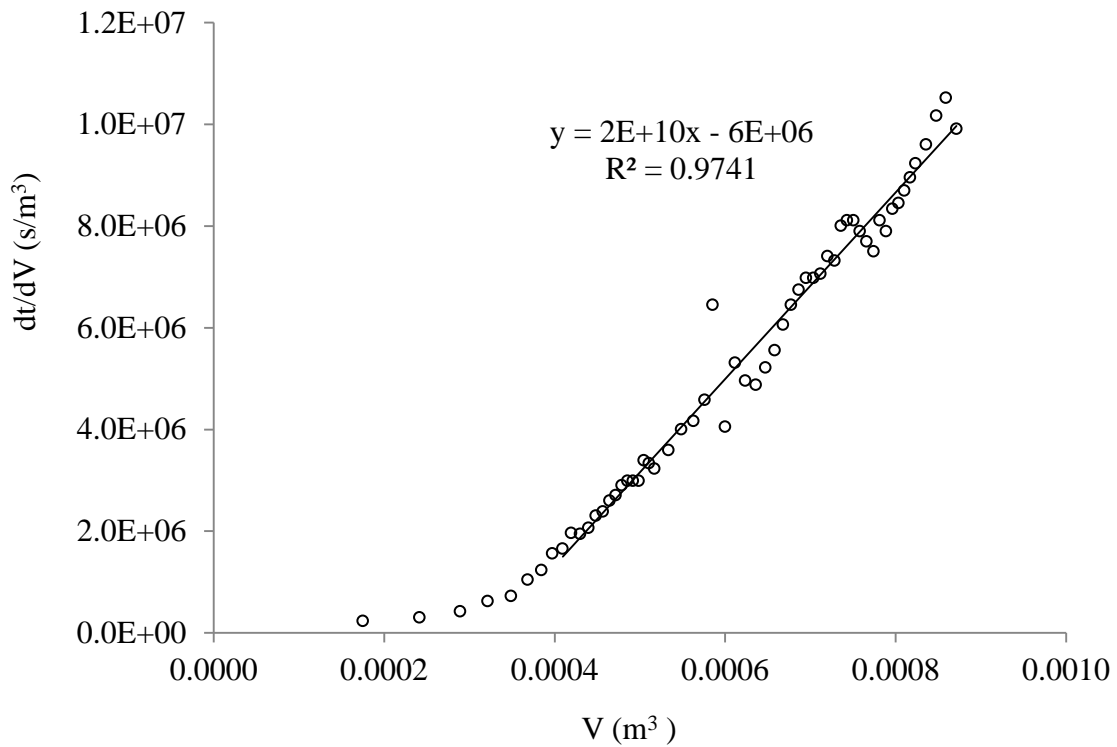


Figure 17. Fouling mechanism identification for the Mixture 1: Cake filtration

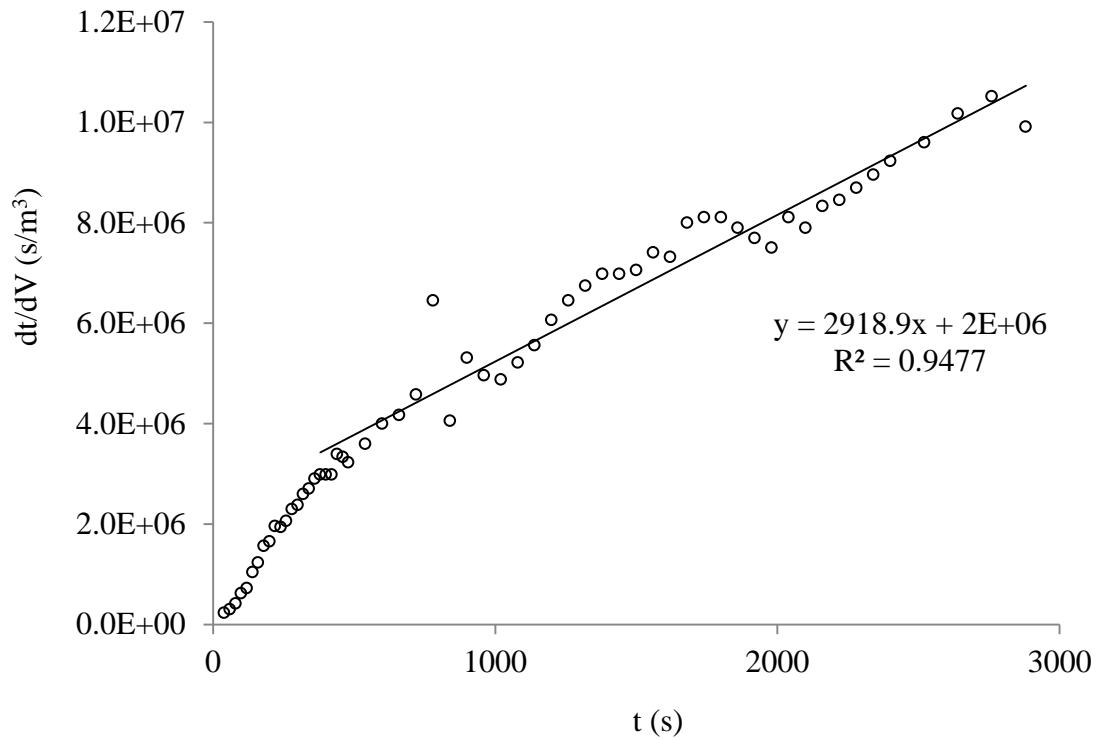


Figure 18. Fouling mechanism identification for the Mixture 1: Intermediate blocking

Identifications of the four fouling mechanisms for the Mixture 2 are included in Figures 19 - 22. The linear regressions in Figure 19 and 20 indicate that standard blocking (pore blocking) and complete blocking (pore constriction) occurred during the filtration experiment with Mixture 2 at a fairly low rates. Furthermore, the slope of these fouling mechanism linear forms identified for Mixture 2 were about 4% of that for Mixture 1, which indicated that no standard blocking and complete blocking happened during filtration of Mixture 2.

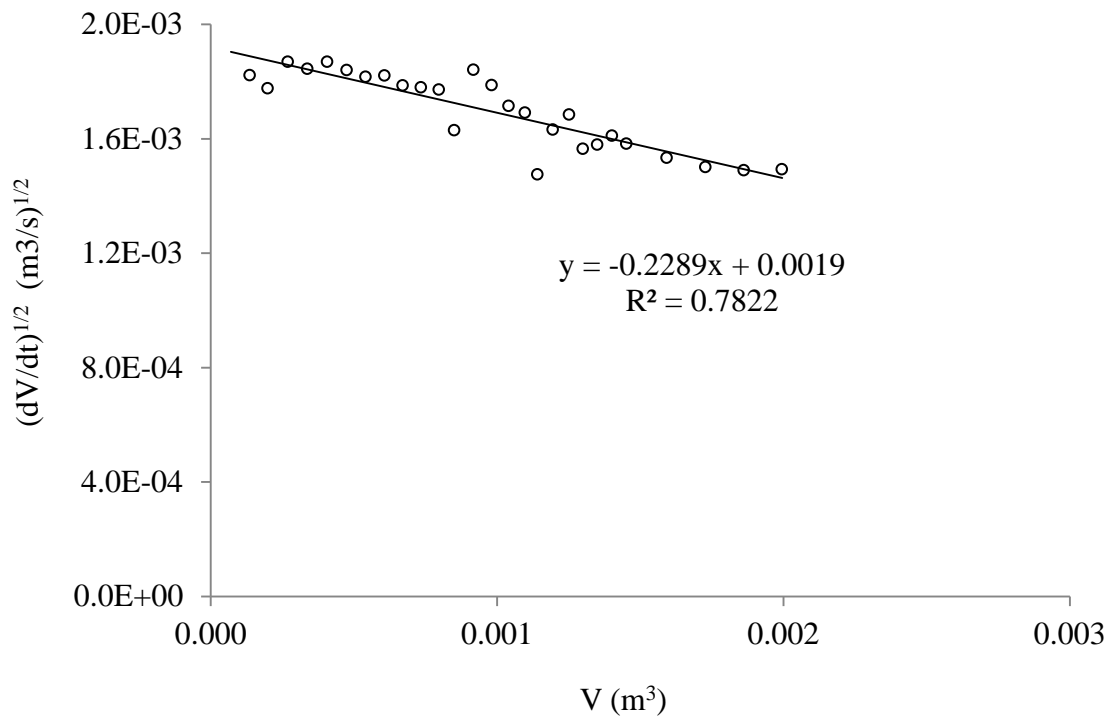


Figure 19. Fouling mechanism identification for the Mixture 2: Standard blocking

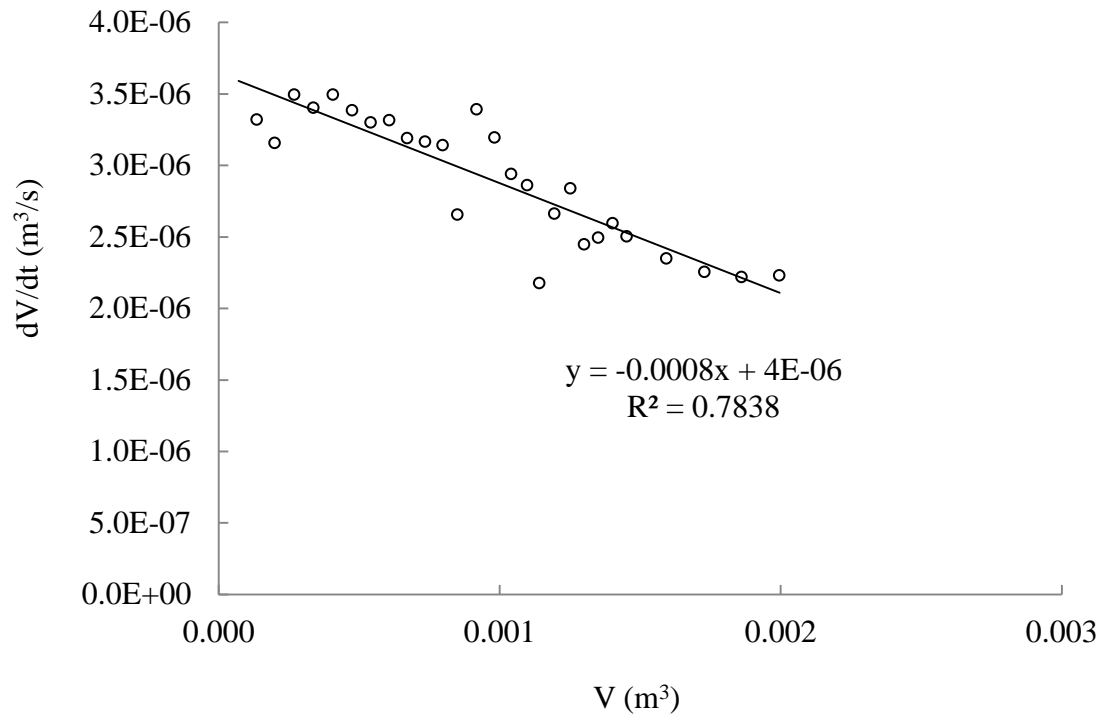


Figure 20. Fouling mechanism identification for the Mixture 2: Complete blocking

In the later stages of filtration for Mixture 2, cake filtration was detected, but the impact was not as significant as in the case of Mixture 1 due to the lower slope of the regression fit and scatter in the data (Figure 21). The intermediate blocking occurred throughout the filtration test but its impact was quite limited, because the regression fit was as low as 0.6 (Figure 22). The slope of intermediate blocking linear form showed continuous increase from the beginning, which indicates built up and aggregation of a cake layer. Thus, cake filtration was the dominant fouling mechanism for Mixture 2.

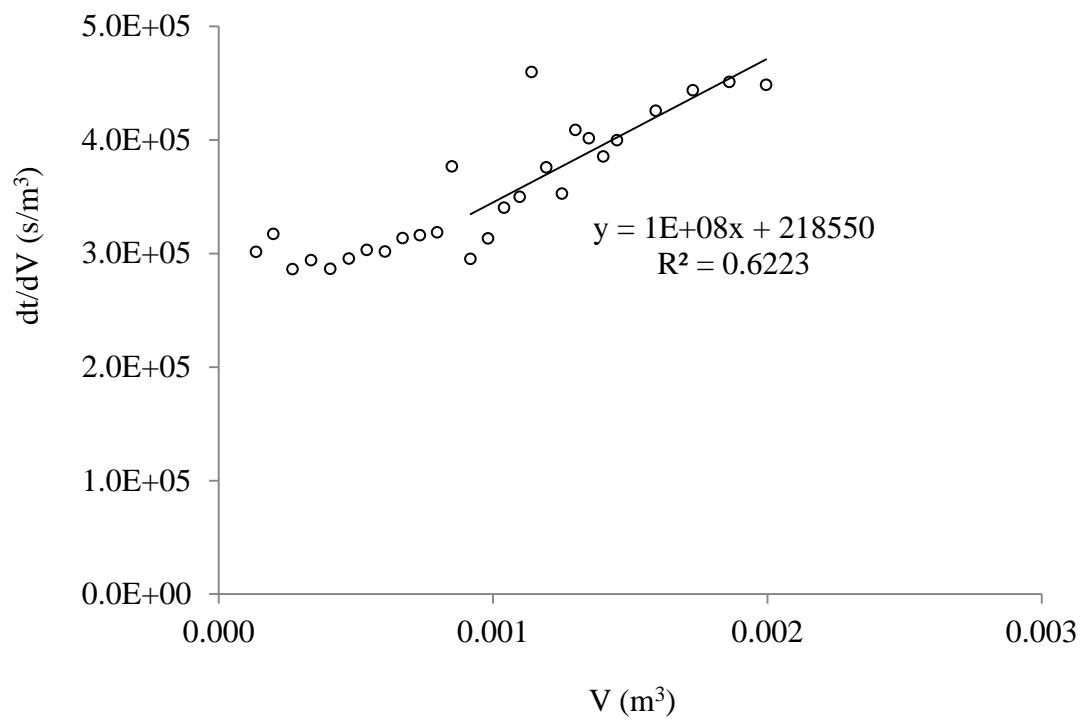


Figure 21. Fouling mechanism identification for the Mixture 2: Cake filtration

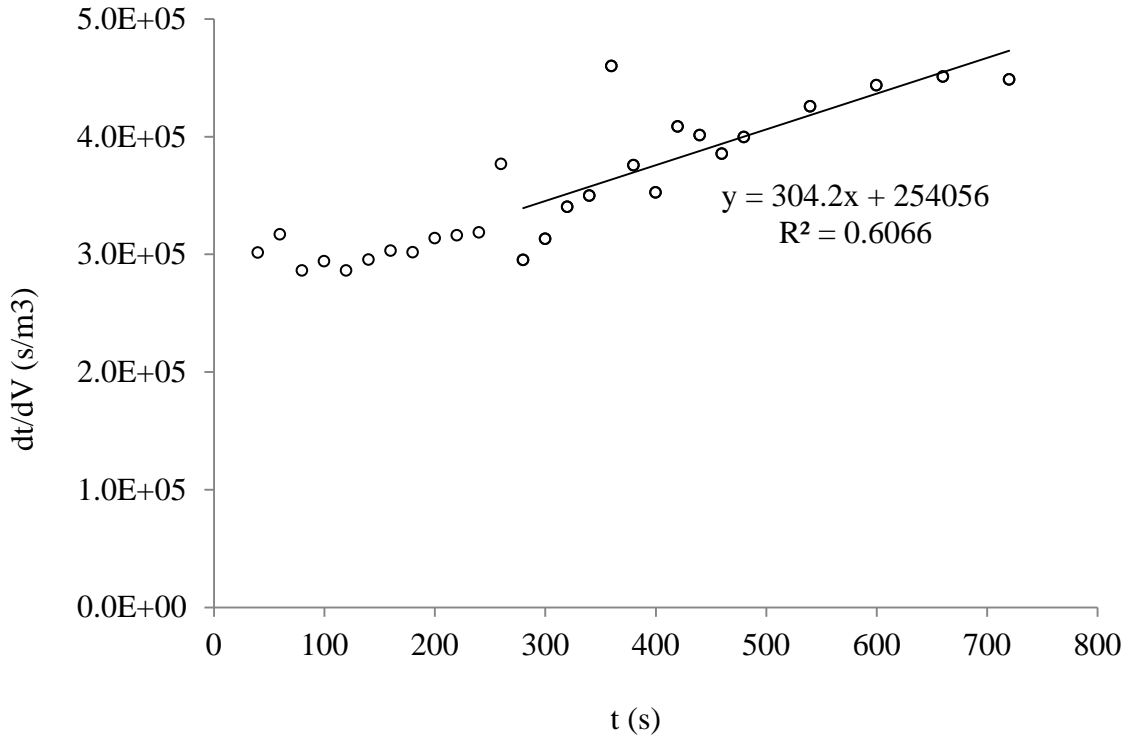


Figure 22. Fouling mechanism identification for the Mixture 2: Intermediate blocking

Filtration test analyses for diluted flowback water and diluted AMDs are summarized in Table 6. The regression coefficients (R^2) for different fouling mechanisms as well as the ranges of filtrate volume (L) for which the regression have been performed are also included in Table 6.

For the diluted Flowback water A, the fouling mechanisms were found to be similar to those detected for Mixture 1. Standard blocking and complete blocking were identified at the beginning of the filtration experiment, followed by the cake filtration in the later stages. This behavior is due to the presence of sub-micron particles in Flowback water A.

For the diluted AMD 1, no dominant fouling mechanism was found and the linear regression coefficients were fairly low for all fouling mechanisms, no significant fouling was observed when compared with Mixture 1 or Flowback water A.

No dominant fouling mechanism was identified for the diluted Flowback water B, which was similar to the results observed for Mixture 2. In the early stages of filtration, no significant standard blocking or complete blocking could be identified. Because the particles in the Flowback water B were larger than the membrane pore size, they were not able to cause pore constriction or pore blocking. Moreover, no sub-micro particles were detected in Flowback water B.

As shown in Table 6, there was no standard blocking (pore constriction) happened during the filtration of diluted AMD 2. This was expected because the AMD 2 contains particulate matter of larger size than the membrane pores and virtually no organic matter. Complete blocking, intermediate fouling and cake formation were observed with AMD 2 only after filtering half of feed solution, which corresponds to a VCF of 2.

Table 6. Fouling mechanism identification data summary for flowback water and AMD

		Mixture 1	Diluted Flowback water A	Diluted AMD 1	Mixture 2	Diluted Flowback water B	Diluted AMD 2
Cake filtration	R^2 V (L) *	0.9741, 0.40~0.90	0.9514, 0.37~0.72	0.67967, Total volume	0.6223, 0.92~2.0	0.9618, Total volume	0.95094, 0.84~end
Intermediate blocking	R^2 V (L) *	0.9477, 0.49~0.87	0.9122, 0.37~0.72	0.6736 Total volume	0.6066, 0.92~2.0	0.9691, Total volume	0.9569, 0.91~end
Standard blocking	R^2 V (L) *	0.9855, 0.18~0.40	0.9780 0~0.24	0.708 Total volume	0.7822, Total volume	0.9746, Total volume	N/A
Complete blocking	R^2 V (L) *	0.9930, 0.18~0.40	0.9907 0~0.22	0.7149 Total volume	0.7838, Total volume	0.9713, Total volume	0.94067, 0.84~end

* V indicated the volume range for which the regression has been determined.

Turbidity, TOC and particle size distribution in all feed waters and filtrates are summarized in Table 7. Due to the low turbidity of both AMD samples, the turbidities of mixtures were much lower than that of flowback waters. In addition, the turbidity removal for Mixture 1 was 45% and that for Mixture 2 was 73%. Mixing of flowback water and AMD successfully reduced the TOC of Flowback water A from 52 to 2.4 mg/L and the TOC of

Flowback water B from 152.7 to 5.1 mg/L, which reduced the potential of membrane fouling by organic matter.

Table 7. Initial turbidity, particle size distribution data summary for flowback water and AMD

	Turbidity (NTU)	TOC (mg/L)	Particles size at peak Number% (μm)
Flowback water A	60	52	3.13 (0.11 [*])
AMD 1	7.4	-	-
Mixture 1	33	2.4	1.3
Flowback water B	18	132.7	8.1
AMD 2	0.5	-	-
Mixture 2	4.9	5.1	11.5

* Small particle size distribution in nanometer range.

To compare the severity of the fouling for membrane filtration experiments of all feed waters, cake volumic specific resistance and complete blocking parameters were calculated and summarized in Table 8. The cake volumic specific resistance η_c (m^{-2}) was calculated based on the following equation (Grenier et al., 2008):

$$\eta_c = \frac{KAP}{\mu} \quad (7)$$

where:

η_c = cake volumic specific resistance (m^{-2})

K = slope of the $dt/dV = f(t)$ line

A = membrane surface area (m^2)

P = applied pressure (Pa)

μ = dynamic viscosity of the permeate (Pa·s)

The complete blocking parameter represents the ratio of the blocked surface area and total membrane surface area η_B (m^{-1}), and is related to the fouling by pore blocking. The complete blocking parameter is expressed by (Grenier et al., 2008):

$$\eta_B = \frac{k_B}{J_0} \quad (8)$$

where:

η_B = blocking parameter (m^{-1})

k_B = slope of the $dV/dt = f(V)$ line

J_0 = initial flux ($L h^{-1} m^{-2}$)

The severity of the membrane fouling is related to the value of the cake volumic specific resistance and the blocked surface area (Grenier et al., 2008).

In Table 8, the cake resistance and blocked surface area were significantly (1-2 orders of magnitude) greater for Flowback water A and Mixture 1 than for Flowback water B and Mixture 2. The high cake resistance for Mixture 1 and Flowback water A may be due to a thick and dense cake that formed on the membrane surface. The higher turbidity in the Flowback water A has the potential to cause the thicker cake deposit than in the Flowback water B. The existence of sub-micron particles in Flowback water A could easily cause membrane pore blocking or constriction in the early stages of filtration process, which explains much faster decrease of permeate flux in Flowback water A than in Flowback water B. Therefore, it was expected that higher cake volumic specific resistances and blocked surface area would be obtained in the filtration process involving Flowback water A than Flowback water B.

Barium sulfate particles played a negligible role in the membrane fouling. The cake volumic specific resistance of both mixtures was slightly lower than that of the flowback waters

(Table 8). These results indicate that slightly looser (less dense) cakes are formed in the presence of barium sulfate crystals.

Both AMDs and Flowback water B created fairly low cake resistances and very limited pore blocking compared to Flowback water A and AMD 1 (Table 8). These results further prove that sub-micro particles in Flowback water A caused pore constriction and pore blocking at the early stages of filtration, which was the main reason for severe membrane fouling by Mixture 1 or diluted Flowback water A.

Table 8. Cake volumic specific resistance, blocking parameter data summary for flowback water and AMD

	Cake volumic specific resistance (m^{-2})	Blocking parameter (m^{-1})
Flowback water A	5.12×10^{15}	(88.9)*
AMD 1	1.36×10^{13}	0.803
Mixture 1	4.05×10^{15}	16.64
Flowback water B	2.49×10^{13}	0.959
AMD 2	9.99×10^{12}	1.504
Mixture 2	2.20×10^{13}	0.916

* Regression was performed on a very limited set of data.

4.2 COAGULATION AND FLOCCULATION

Coagulation is defined as the process to destabilize the colloidal and fine suspended solids. Flocculation is the slow stirring or gentle agitation to aggregate the destabilized particles and form a rapid settling floc (Reynolds and Richards, 1995). A series of coagulation - flocculation experiments was performed to find out the optimal coagulant type and dosage for turbidity and TOC removal in the mix of flowback water and AMD. The turbidity removal efficiency in coagulation – flocculation - sedimentation was compared with that observed in membrane filtration.

Observation of floc formation is normally used to narrow down the dosage range. The addition of appropriate amount of coagulant will form flocs settle to the bottom leaving clear water on the top (Howe and Clark, 2002). Turbidity and TOC of the supernatant were measured to find out the optimal coagulant type and dosage for each mixture.

Aluminium chloride and ferric chloride were both effective for coagulation - flocculation of Mixtures 1 and 2. The turbidity of both Mixture 1 and Mixture 2 was reduced to below 1.0 NTU (Figure 23 - 26). For engineering application purpose, pH is a critical factor besides turbidity or TOC removal efficiency when choosing the optimal dosage for coagulation – flocculation process. Since the pH for Mixture 1 and 2 were around 7, the optimal dosage at pH of 7 would be the best choice. Comparing Figure 23 and 24, which show the final turbidity, final TOC and the coagulation pH, it is concluded that the optimal coagulant was ferric chloride, at a dosage of 30mg/L at pH=6 for Mixture 1, and at a dosage of 20mg/L at pH=6 for Mixture 2.

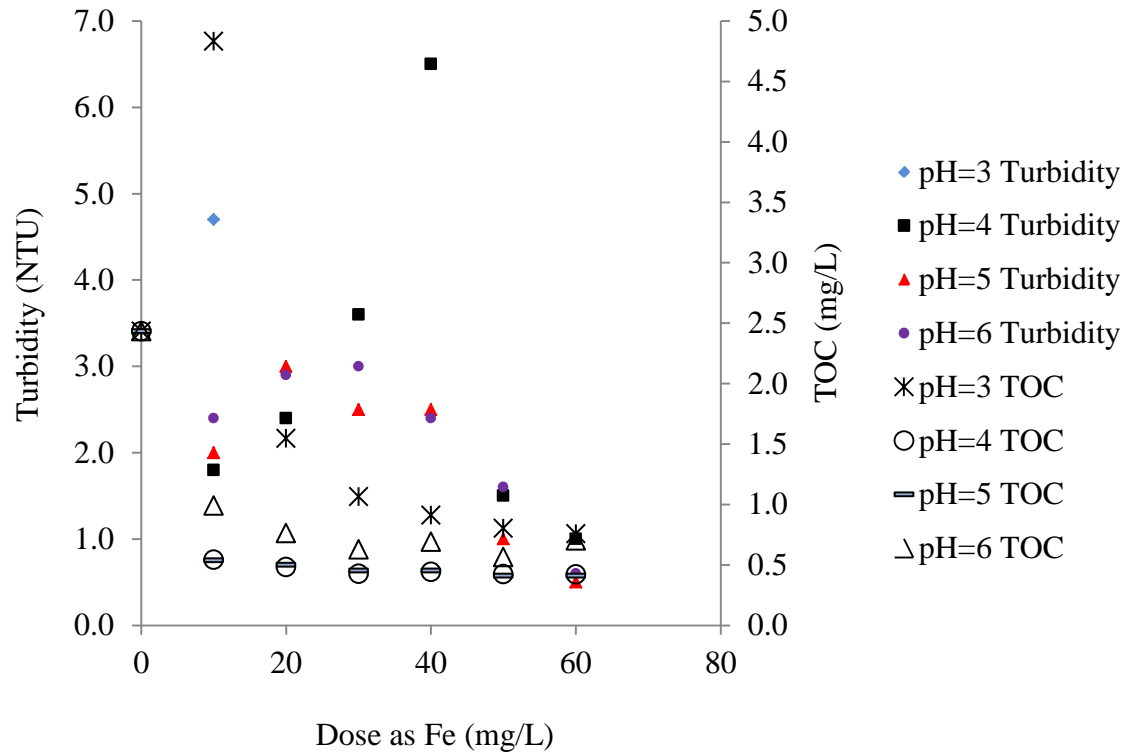


Figure 23. Residual turbidity and TOC as a function of iron dose for Mixture 1 (initial turbidity = 33 NTU, initial TOC = 2.4 mg/L)

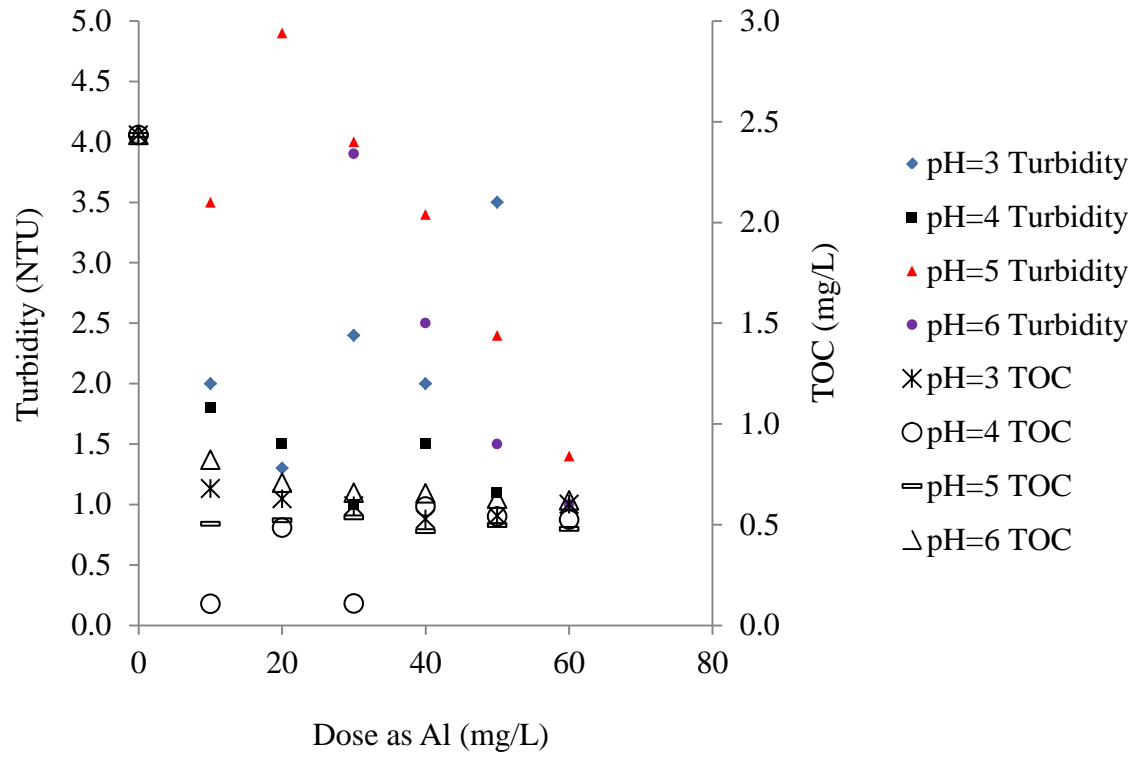


Figure 24. Residual turbidity and TOC as a function of aluminium dose for Mixture 1 (initial turbidity = 33 NTU, initial TOC = 2.4 mg/L)

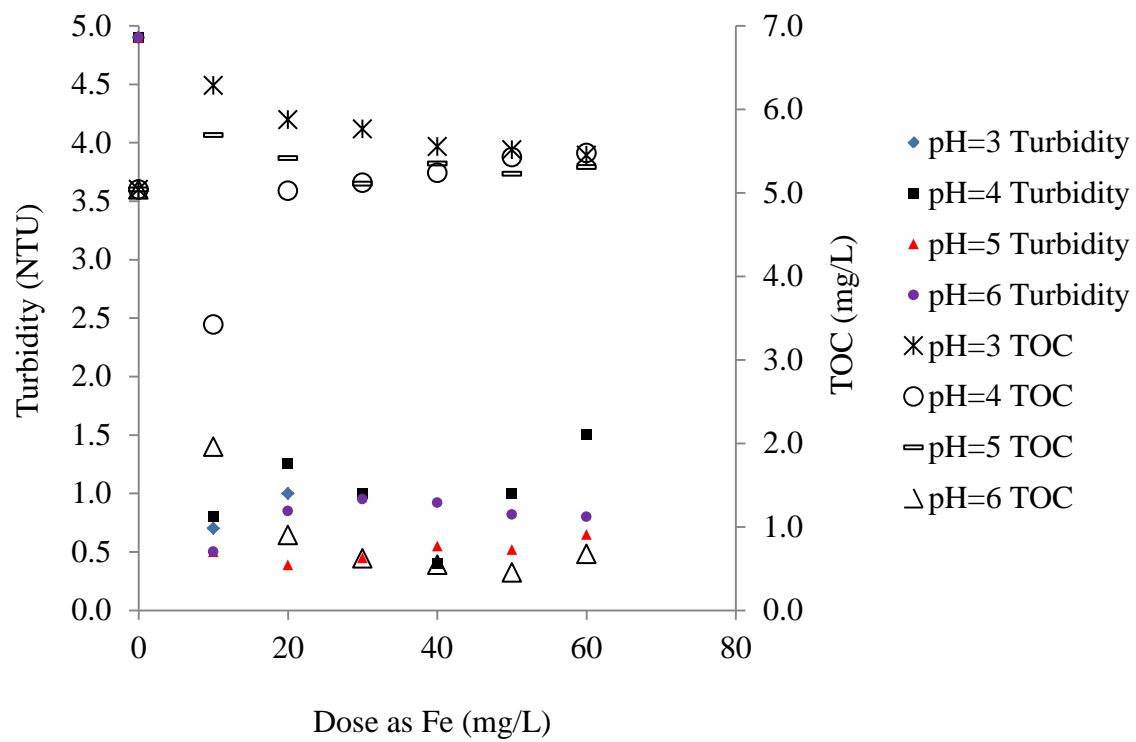


Figure 25. Residual turbidity and TOC as a function of iron dose for Mixture 2 (initial turbidity = 4.9 NTU, initial TOC = 5.0 mg/L)

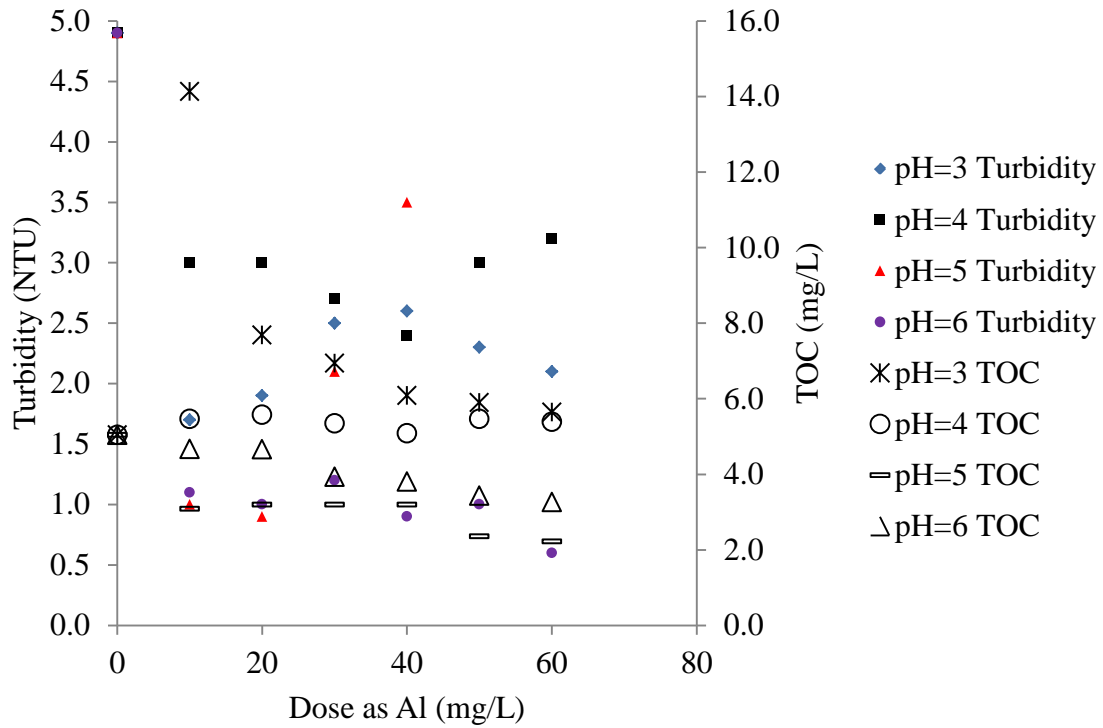


Figure 26. Residual turbidity and TOC as a function of aluminium dose for Mixture 2 (initial turbidity = 4.9 NTU, initial TOC = 5.0 mg/L)

The best turbidity and TOC removal efficiencies for Mixture 1 and 2 are summarized in Table 9. Optimal dosages of aluminium chloride and ferric chloride for coagulation of Mixtures 1 and 2 are listed in Table 10.

Table 9. Summary of turbidity and TOC removal by coagulation-flocculation-sedimentation

	FeCl ₃ ·6H ₂ O (as Fe)	AlCl ₃ ·6H ₂ O (as Al)
Mixture 1 turbidity removal (%)	91	97
Mixture 1 TOC removal (%)	74	96
Mixture 2 turbidity removal (%)	83	82
Mixture 2 TOC removal (%)	82	37

Table 10. Summary of optimal coagulant dosages

	FeCl ₃ ·6H ₂ O (as Fe)	AlCl ₃ ·6H ₂ O (as Al)
Mixture 1	30 ± 5 mg/L, pH=6	30 ± 5 mg/L, pH=4
Mixture 2	20 ± 5 mg/L, pH=6	20 ± 5 mg/L, pH=5

The optimal coagulant dosages and pH values for both Mixture 1 and Mixture 2 are included in Table 11 together with turbidity changes by precipitation due to mixing with AMD, membrane filtration and coagulation – flocculation - sedimentation. Turbidity removal efficiencies achieved in membrane filtration and coagulation – flocculation - sedimentation processes were very similar, which shows the potential of using membrane filtration as a replacement for conventional treatment process.

Table 11. Summary of turbidity removed through precipitation, membrane filtration and coagulation - flocculation

	Initial turbidity (NTU)	Turbidity after precipitation with AMD (NTU)	Turbidity after membrane filtration (NTU)	Turbidity after coagulation-flocculation (NTU)
Flowback water A	60	33	1.0	3.0 (Fe, 30mg/L, pH=6)*
Flowback water B	18	4.9	0.2	0.9 (Fe, 20mg/L, pH=6)*

*Residual turbidity with optimal dosage for the mixture.

5.0 SUMMARY AND CONCLUSIONS

Flowback water generated by hydraulic fracturing during shale gas drilling can be reused for subsequent fracturing process. AMD is a water source that is often located in the vicinity of gas wells and can be mixed with flowback water to reduce the water usage for hydraulic fracturing. A bench-scale dead-end microfiltration unit was used for filtration experiments with GVWP (Milipore) membrane for flowback water treatment. Mixing of AMD with flowback water leads to precipitation of Ba, Ca and Sr as sulfates. Mixing flowback water with AMD overnight (~12 hours) before membrane filtration successfully reduced the turbidity and TOC, and formed larger particles that had lower impact on membrane fouling.

Severe membrane fouling occurred after few minutes of Mixture 1 filtration, which was due to the sub-micron particles in Flowback water A. The particle size distribution analysis of the Flowback water A filtered through 0.45 μm membrane showed a peak particle size of 0.11 μm . Thus, the particles with a size close to the membrane pore diameter led to pore constriction and pore blocking during filtration of Mixture 1 or diluted Flowback water A. Furthermore, the standard blocking (pore constriction) was identified as a dominant fouling mechanism in the early stages of filtration. On the contrary, no severe fouling was found during filtration of Mixture 2, since the bigger particles in Flowback water B had less impact on membrane fouling.

Barium sulfate precipitate plays negligible role in membrane fouling. The filtration of two barium sulfate solutions containing an order of magnitude different concentration showed

identical permeate flux behavior. Moreover, slightly lower cake resistance was measured in the presence than in the absence of barium sulfate crystals.

Aluminium chloride and ferric chloride are effective coagulants in removing turbidity and TOC from Mixture 1 and 2 through coagulation – flocculation - sedimentation. Based on the turbidity and TOC removal efficiency, the optimal coagulant for Mixture 1 was ferric chloride at a dosage of 30mg/L at pH=6 and for Mixture 2 was ferric chloride at a dosage of 20mg/L at pH=6.

In addition, membrane filtration and coagulation – flocculation - sedimentation process showed similar turbidity removal efficiency around 90% in treatment of Mixture 1 or Mixture 2. This finding indicates the potential of using membrane filtration as a replacement for conventional treatment process.

Membrane filtration has the potential to be applied in treatment of flowback water. This technology is capable of removing particles from flowback water. However, the fouling problems may limit its application due to the cost of cleaning process. Adding pre-treatment process is a common method to reduce the membrane fouling, which could include coagulation – flocculation - sedimentation process. Further research is needed to find optimal design and operating parameters for membrane filtration application in flowback water reuse.

6.0 RECOMMENDATIONS FOR FUTURE WORK

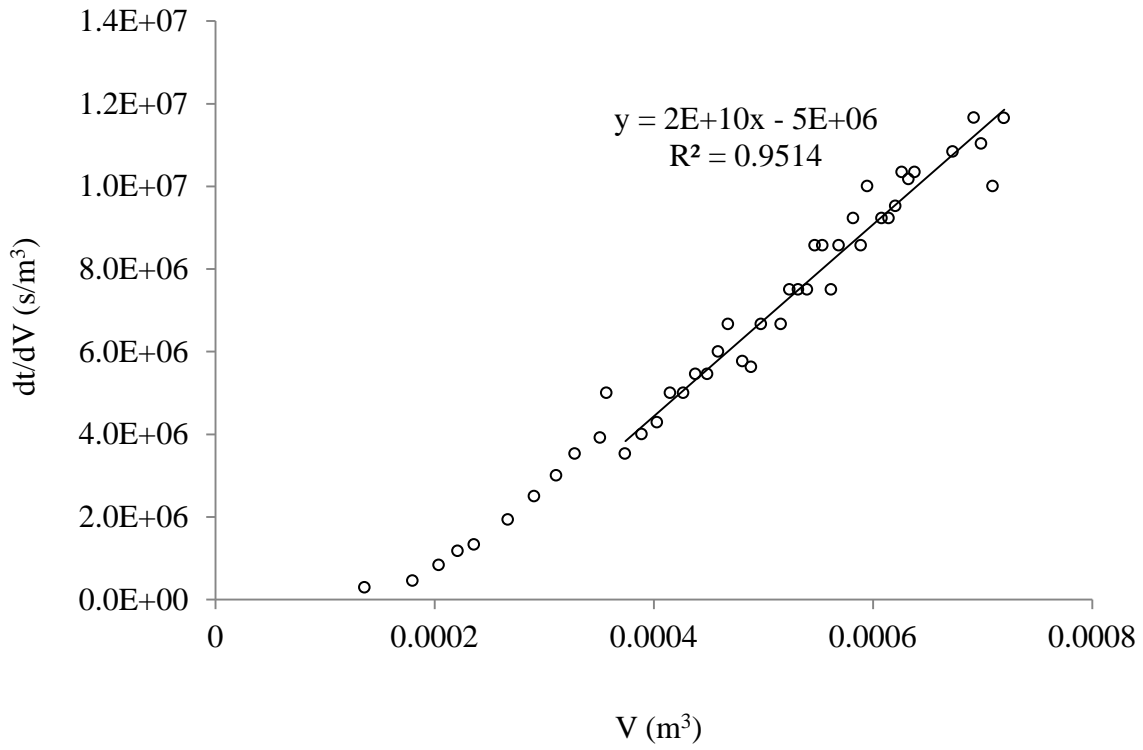
Due to the fact that severe membrane fouling occurred by sub-micron particles in solution, the suggestion to improve the membrane filtration process should focus on pre - treatment or proper selection of the pore size of the membrane. Since the treated flowback water will only be used for subsequent hydraulic fracturing, the quality of the effluent from the membrane filtration process should be defined in terms of well permeability reduction by the particles that are present in the fracturing fluid.

Ultrafiltration may be an option for particle removal from flowback water in the field. Ultrafiltration membrane has the potential to avoid fouling with small particles. Also, coagulation - flocculation - filtration process could be considered as a viable process. The comparison of commercial coagulation - filtration hybrid system and membrane filtration in terms of cost and footprint is necessary.

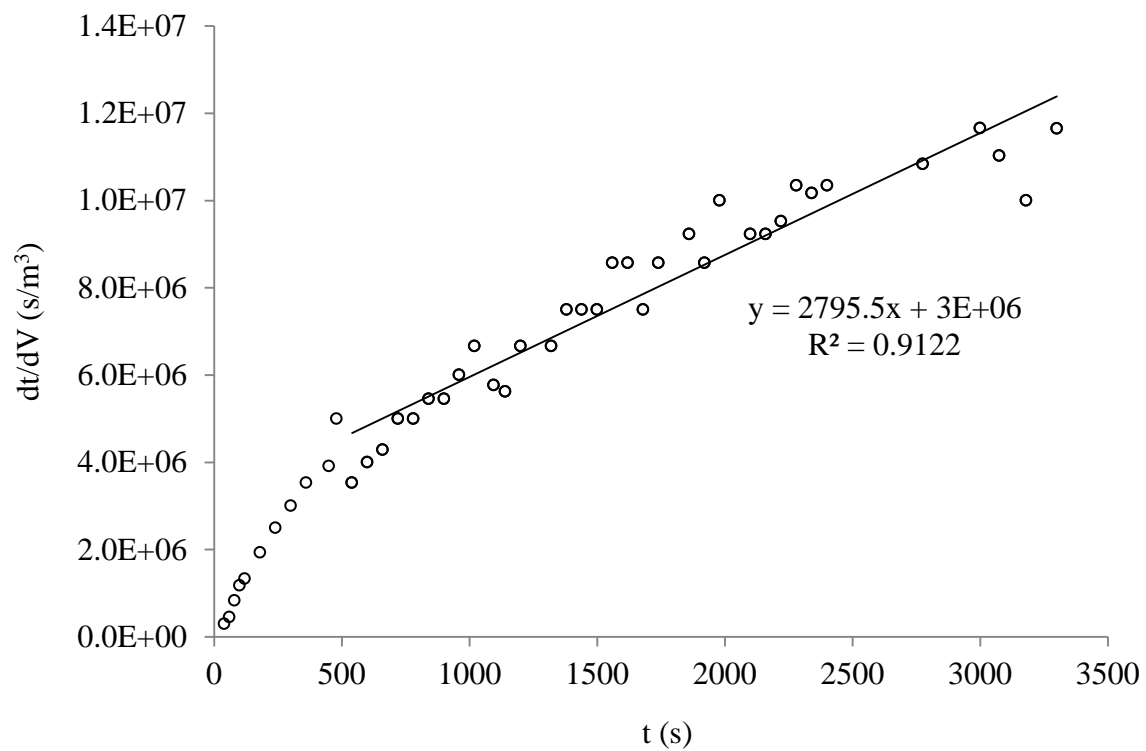
Further research is necessary to fully understand the applicability of microfiltration for a variety of flowback waters since Flowback water A evaluated in this study may be unique in its ability to foul microfiltration membrane. If a flowback water behaves like Flowback water B, microfiltration could be used to treat this flowback water.

APPENDIX A

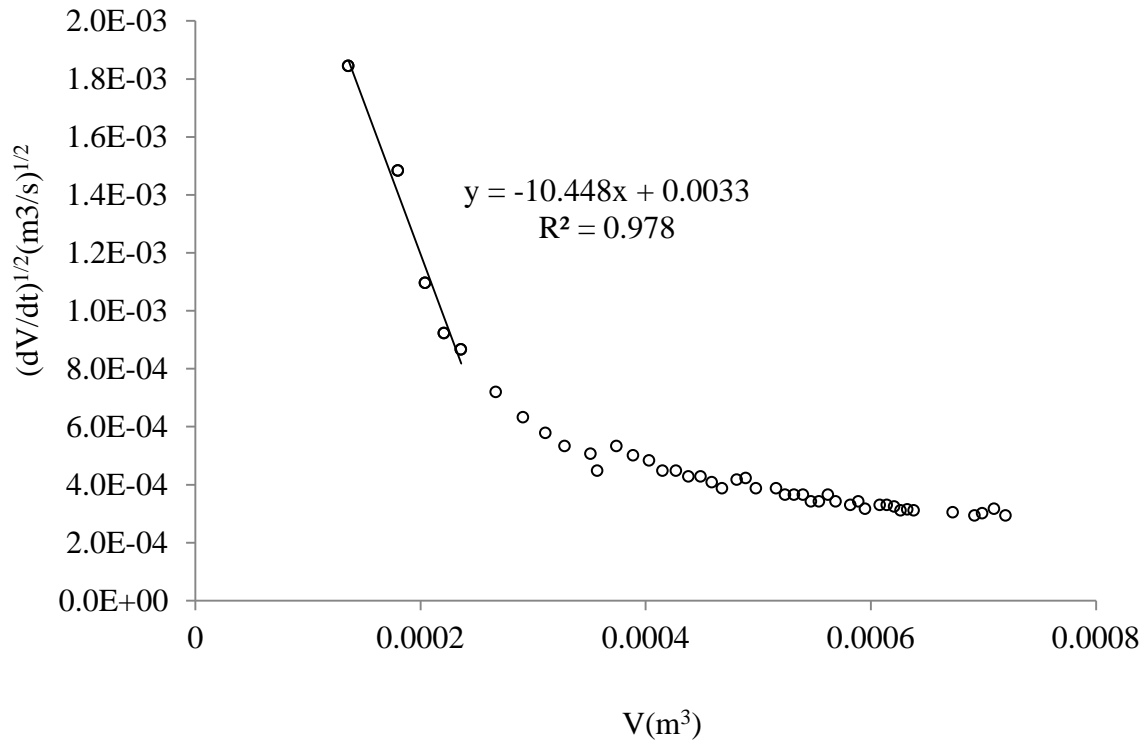
FOULING MECHANISM IDENTIFICATION RESULTS



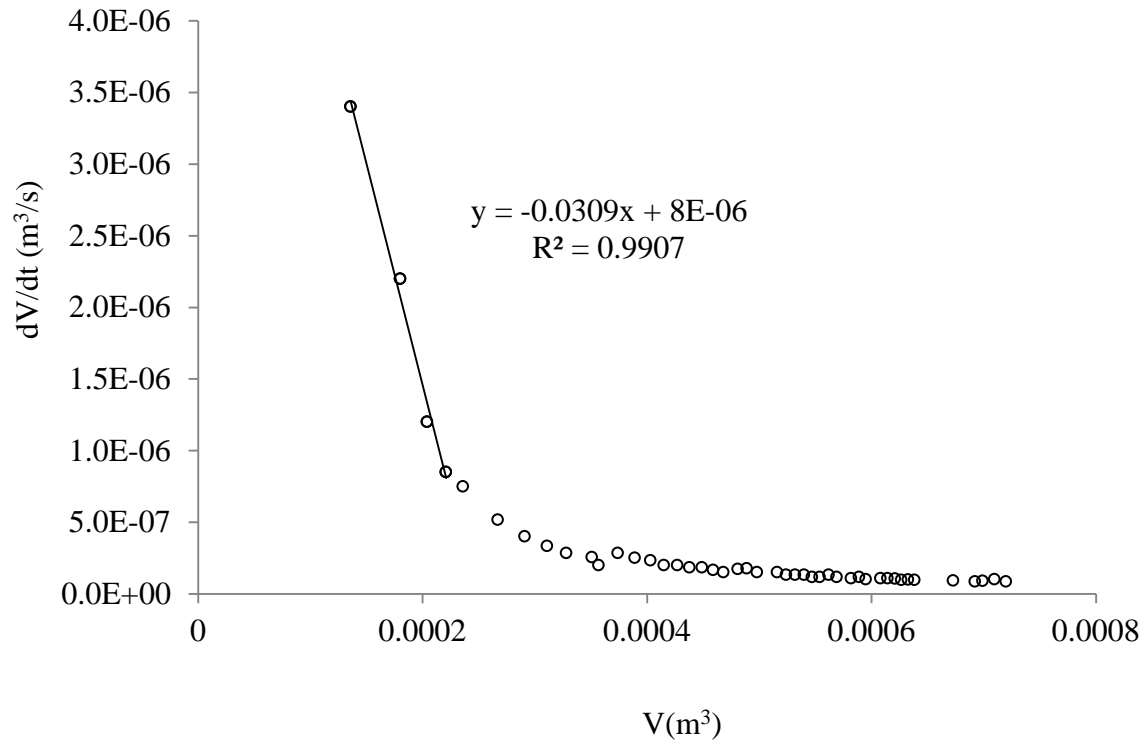
Appendix-Figure 1. Fouling mechanism identification for the Flowback water A: Cake filtration



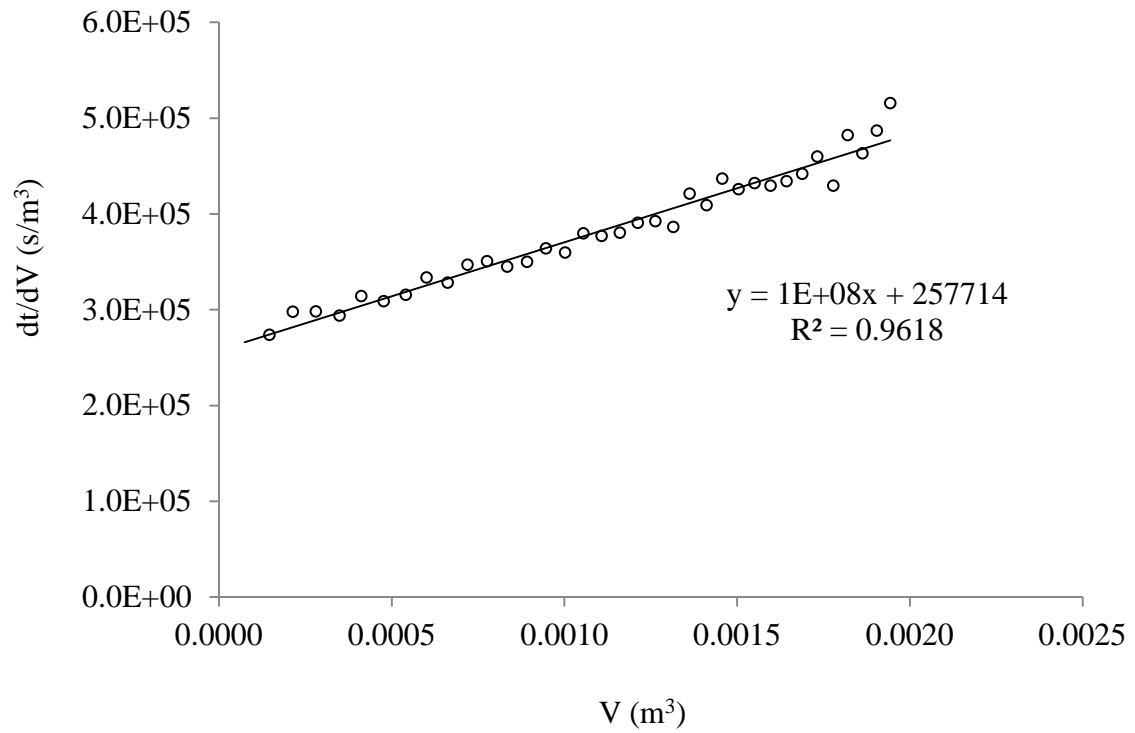
Appendix-Figure 2. Fouling mechanism identification for the Flowback water A: Intermediate blocking



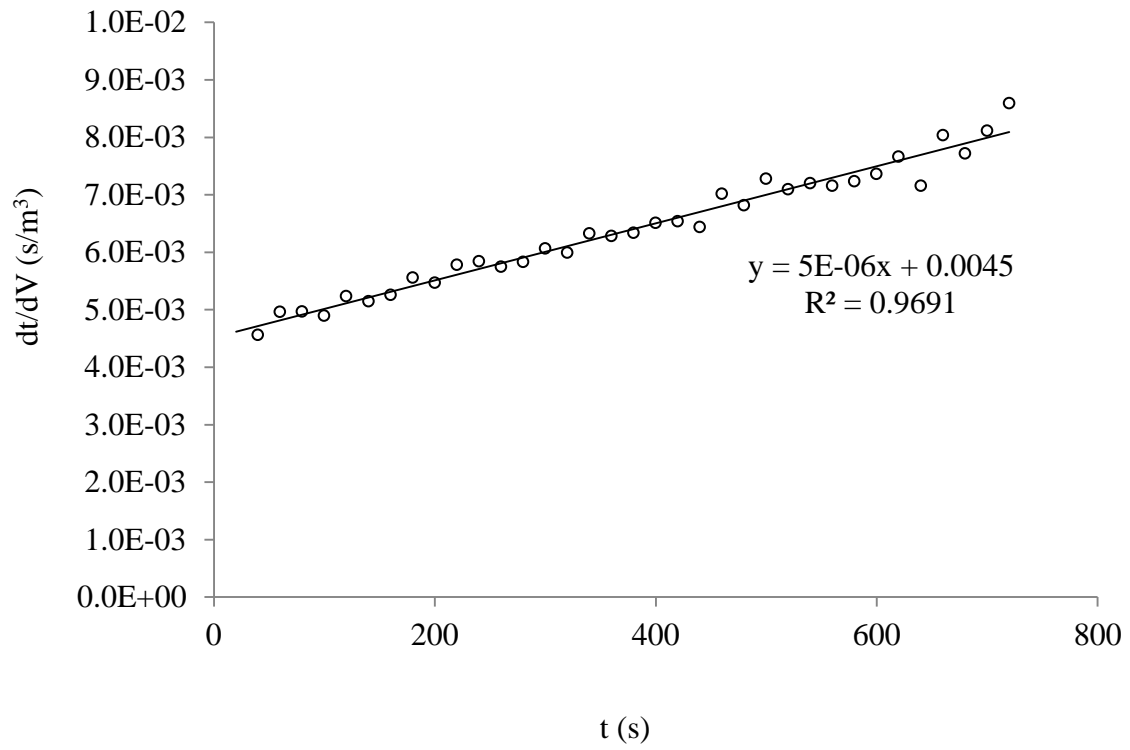
Appendix-Figure 3. Fouling mechanism identification for the Flowback water A: Standard blocking



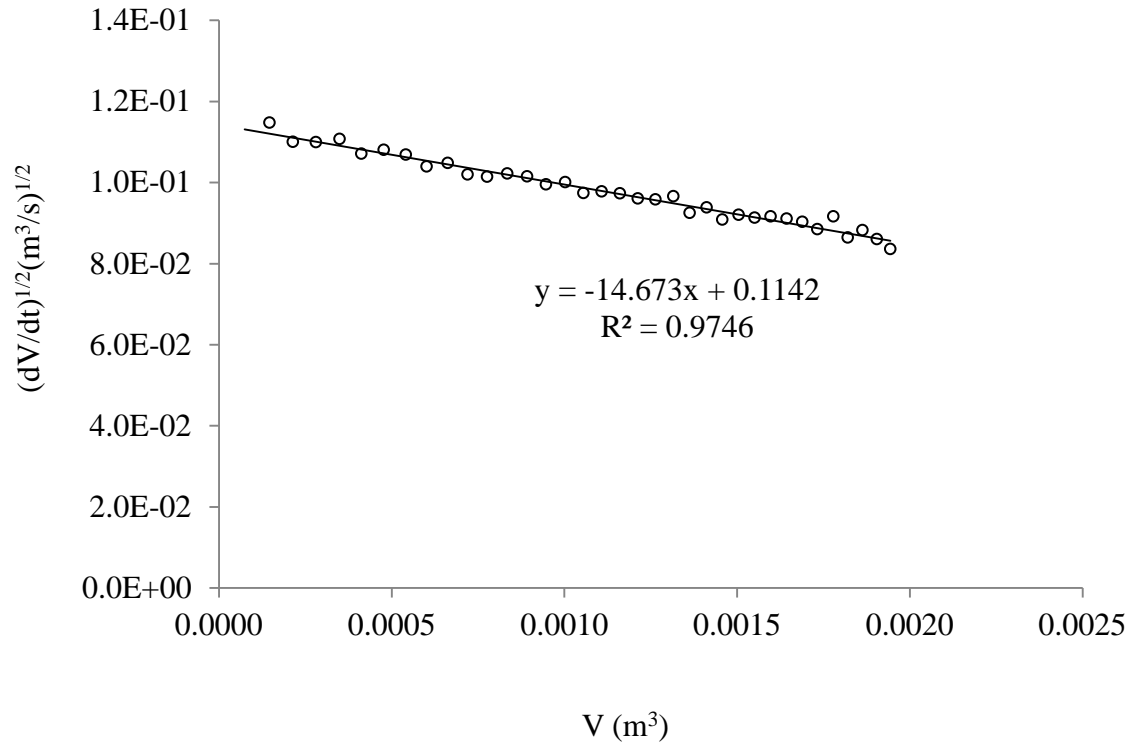
Appendix-Figure 4. Fouling mechanism identification for the Flowback water A: Complete blocking



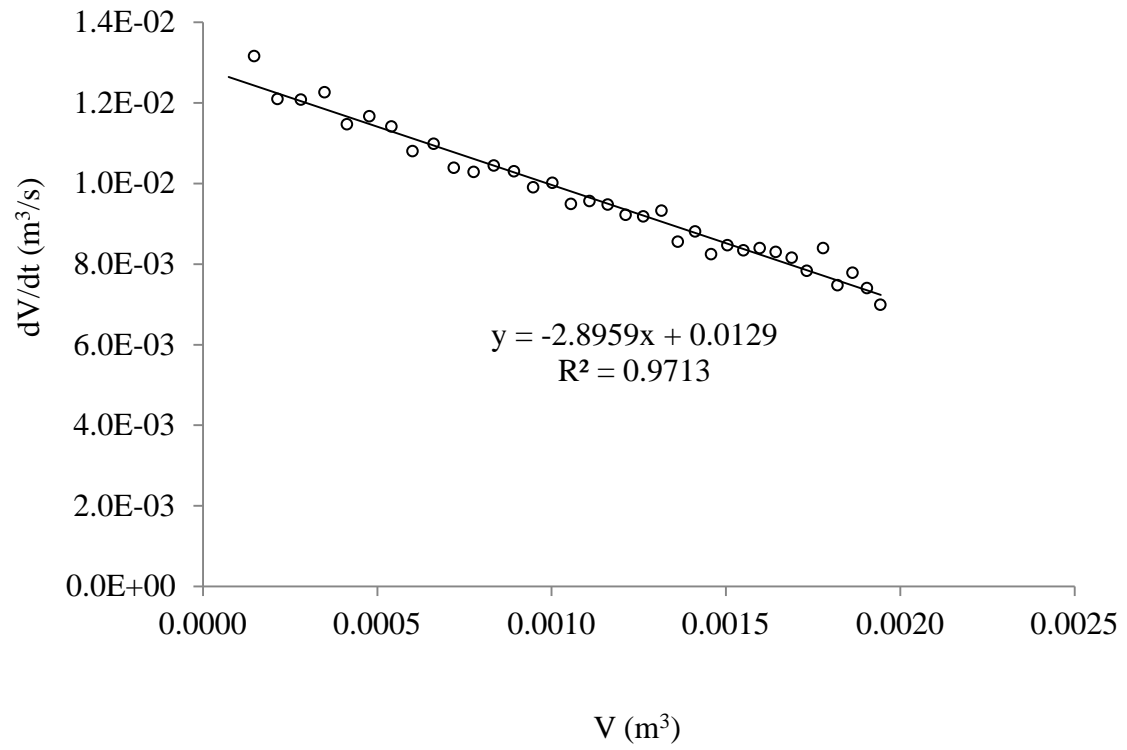
Appendix-Figure 5. Fouling mechanism identification for the Flowback water B: Cake filtration



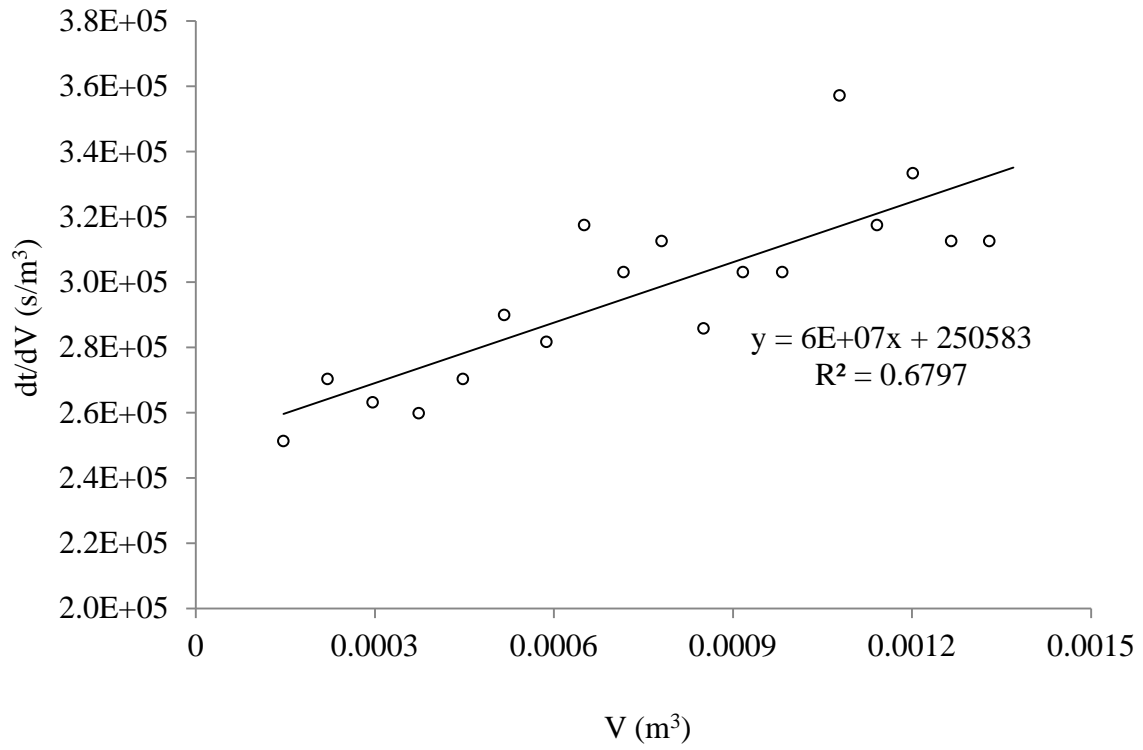
Appendix-Figure 6. Fouling mechanism identification for the Flowback water B: Intermediate blocking



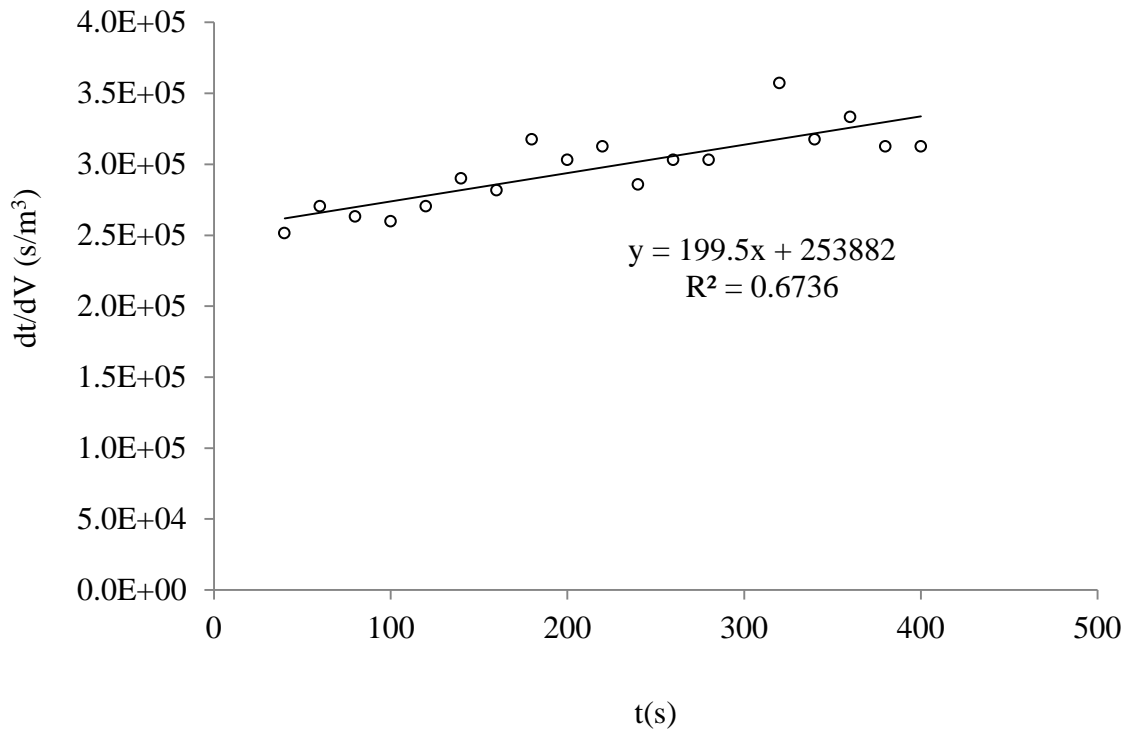
Appendix-Figure 7. Fouling mechanism identification for the Flowback water B: Standard blocking



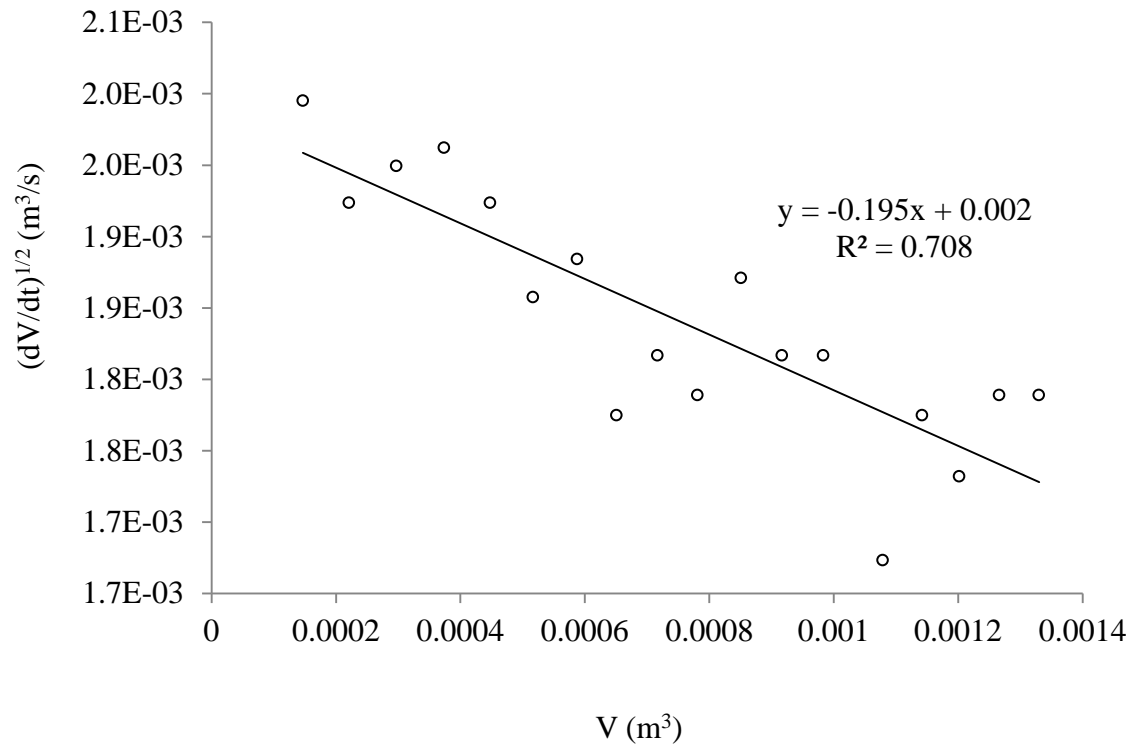
Appendix-Figure 8. Fouling mechanism identification for the Flowback water B: Complete blocking



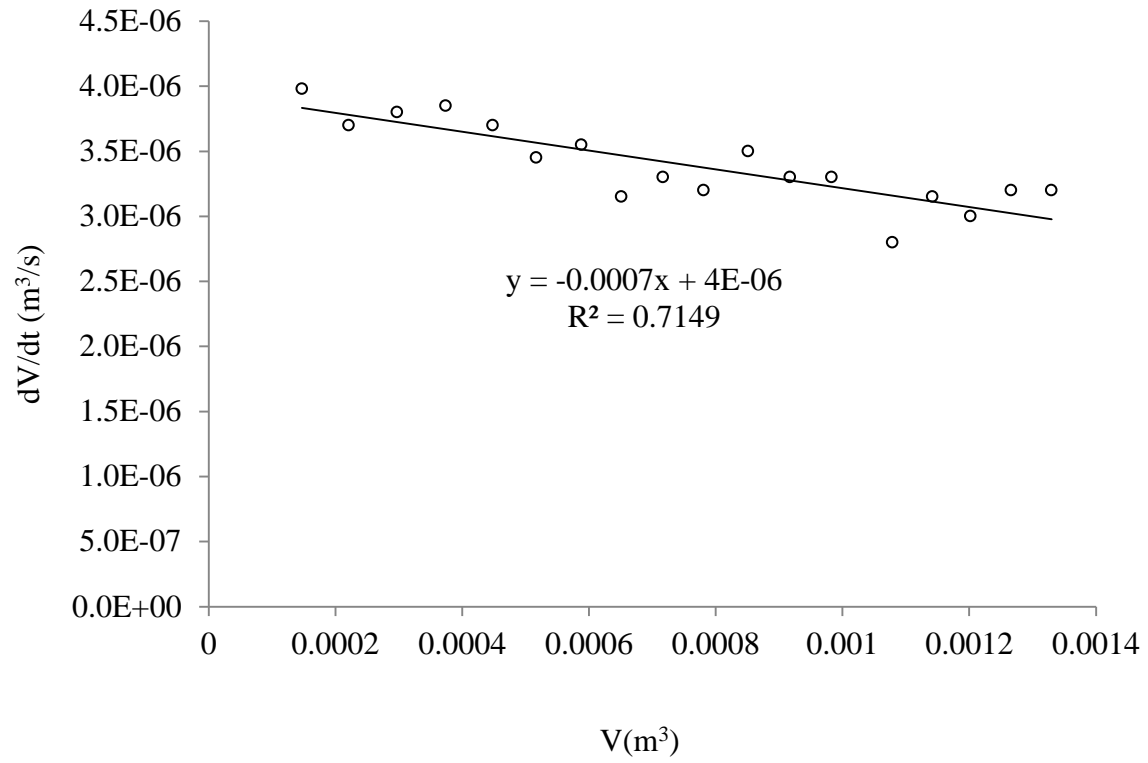
Appendix-Figure 9. Fouling mechanism identification for the AMD 1: Cake filtration



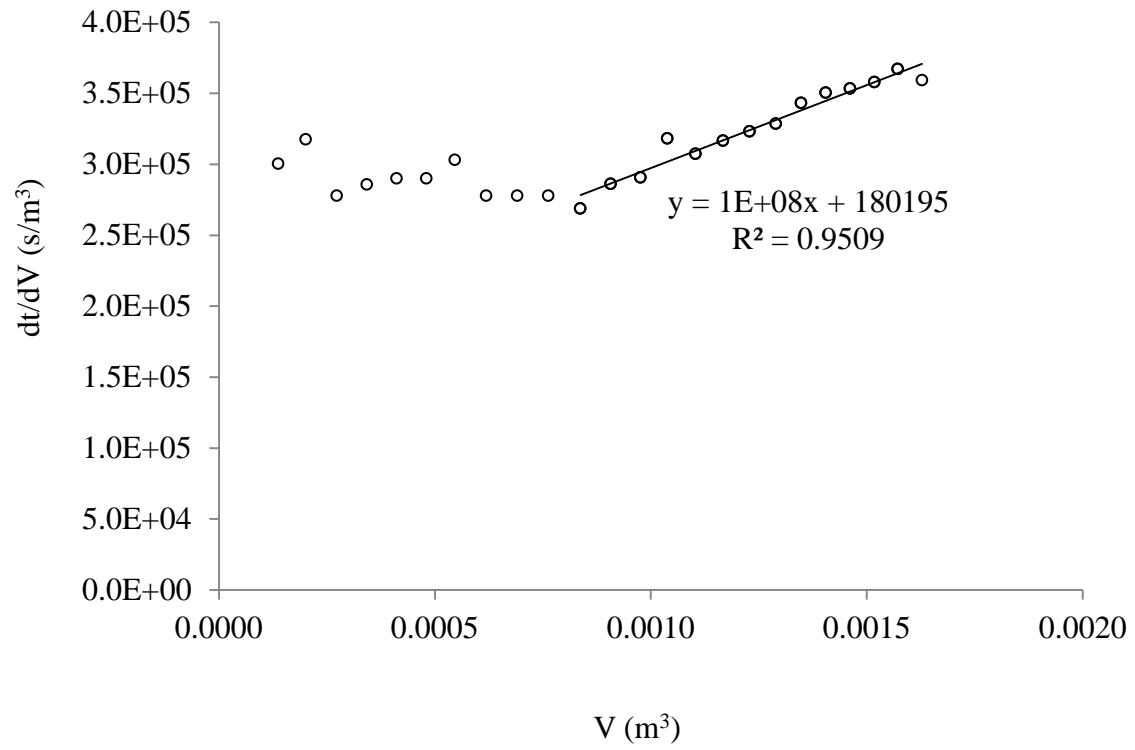
Appendix-Figure 10. Fouling mechanism identification for the AMD 1: Intermediate blocking



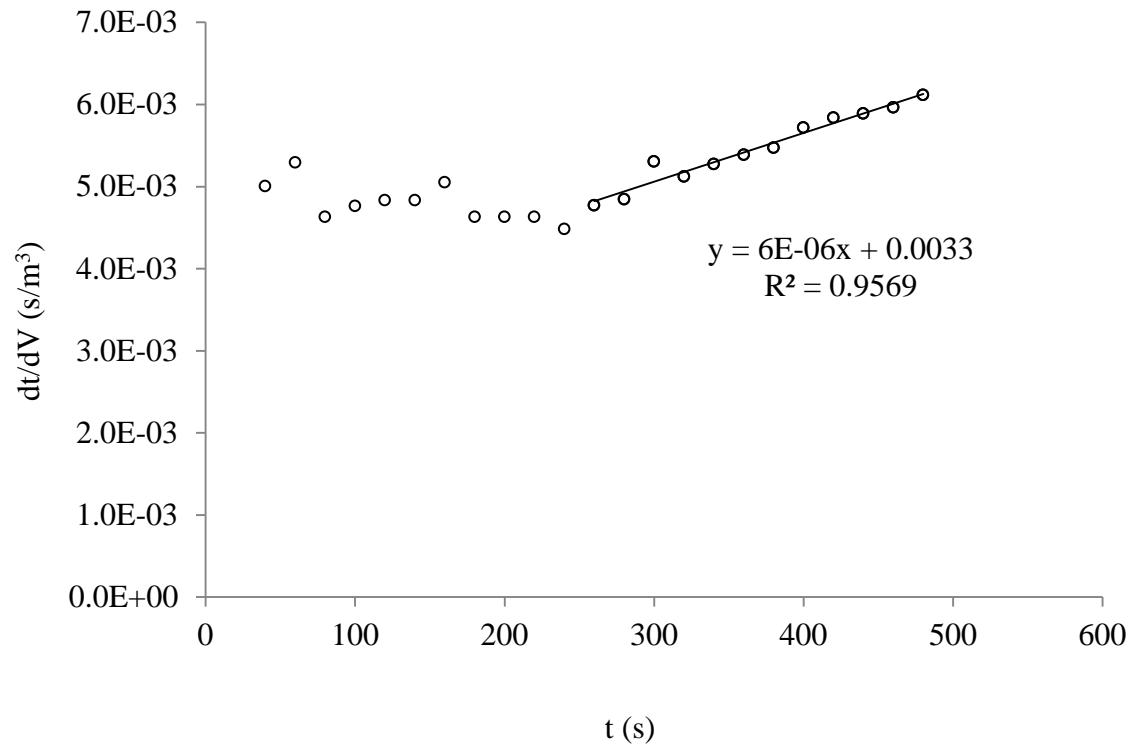
Appendix-Figure 11. Fouling mechanism identification for the AMD 1: Standard blocking



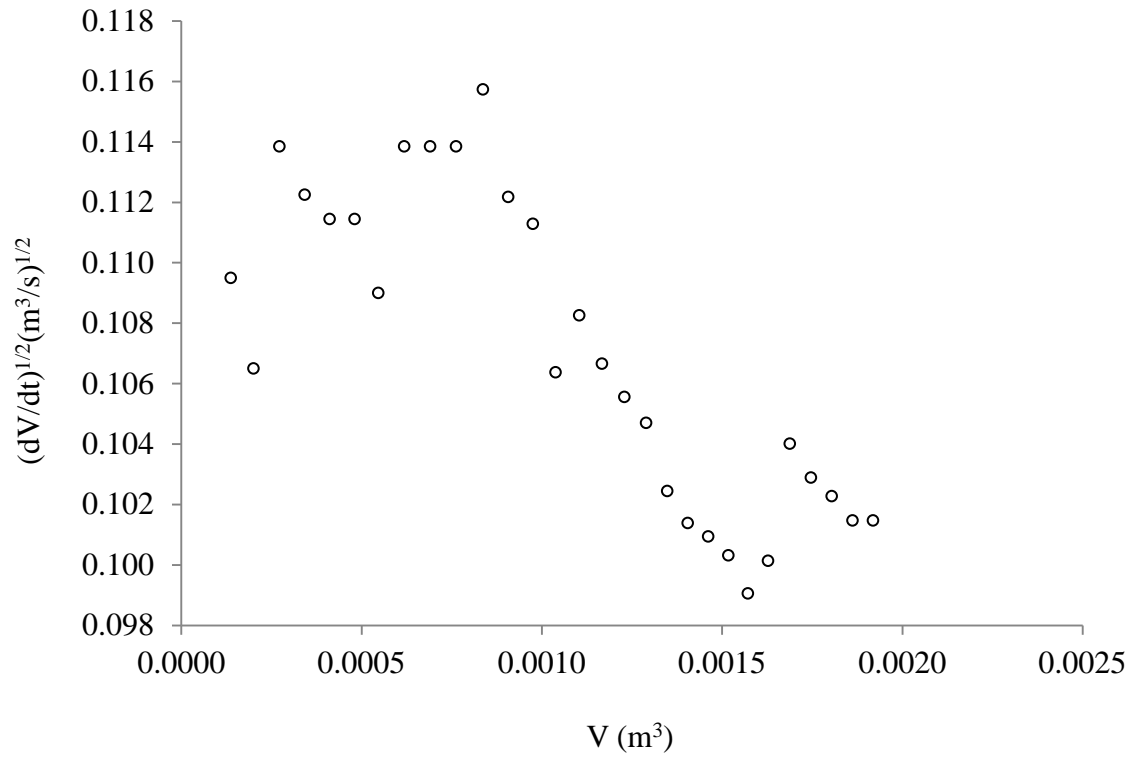
Appendix-Figure 12. Fouling mechanism identification for the AMD 1: Complete blocking



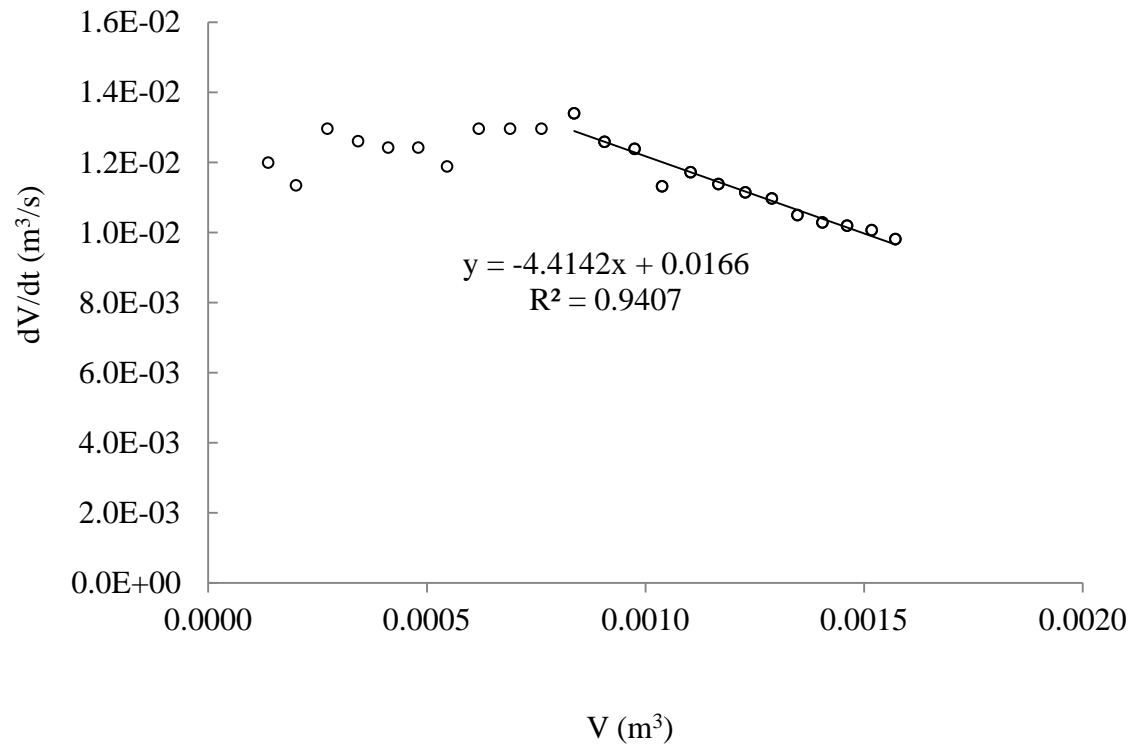
Appendix-Figure 13. Fouling mechanism identification for the AMD 2: Cake filtration



Appendix-Figure 14. Fouling mechanism identification for the AMD 2: Intermediate blocking



Appendix-Figure 15. Fouling mechanism identification for the AMD 2: Standard blocking



Appendix-Figure 16. Fouling mechanism identification for the AMD 2: Complete blocking

APPENDIX B

COAGULATION – FLOCCULATION FOR MIXTURE 1 USING PDADMAC

PDADMAC was evaluated for coagulation – flocculation for Mixture 1.

Appendix-Table 1. Coagulants initial added dose and pH adjustment

PDADMAC*	
Added dose (mg/L)	1, 5, 9, 13, 17, 21
pH	3, 4

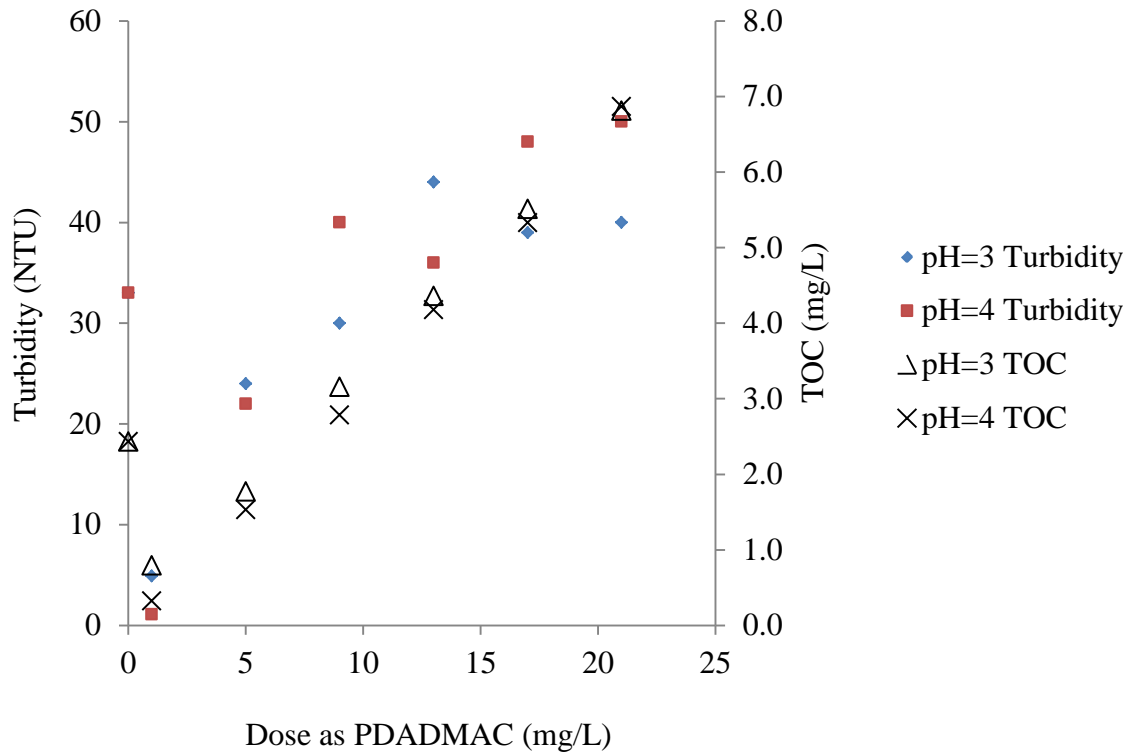
* The PDADMAC was supplied as viscous liquid of 20 wt. % in H₂O with an average MW of 400,000-500,000 which is in a range of high molecular weight.

As shown on Appendix-Figure 17 optima dosage for PDADMAC was found to be relatively low, since the best turbidity and TOC removals were observed at less than 1 mg/L. Further optimization of PDADMAC dosage was performed for lower dosages, and Appendix-Figure 18 and 19 show that the highest turbidity and TOC removal for Mixture 1 were 90.9% and 68.19% respectively, at PDADMAC dosage of 0.7 mg/L at pH 3.

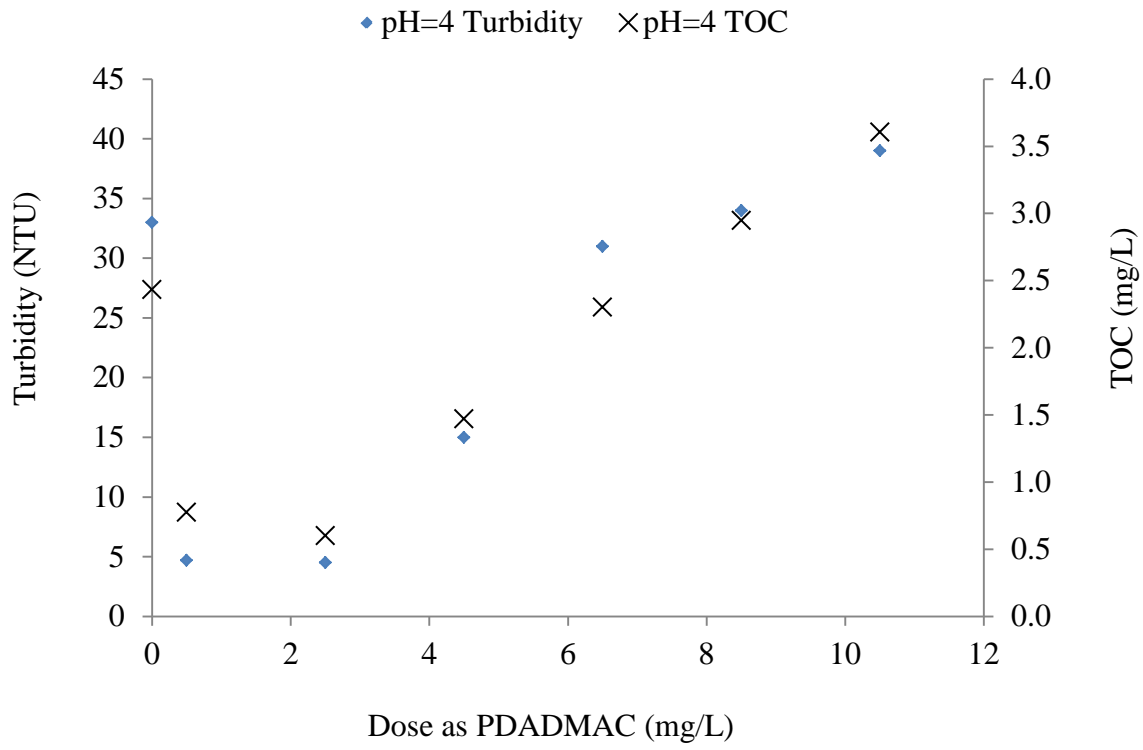
However, turbidity of Mixture 1 was only reduced to 3 NTU using the coagulation with PDADMAC, which is much higher final turbidity when compared with the results from coagulation - flocculation using aluminium chloride and ferric chloride. The optimal pH value

was 3, which requires relatively large acid usage, since the initial pH of the Mixture 1 was around 7.

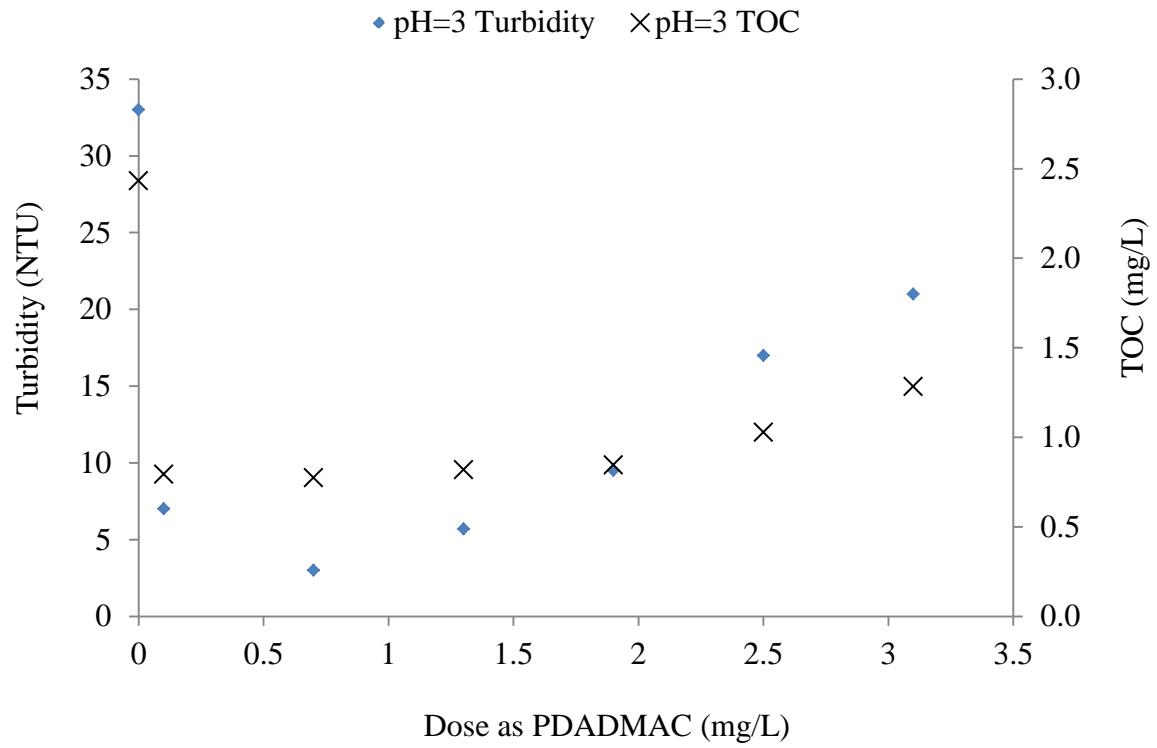
In conclusion, PDADMAC was not as effective as aluminium chloride and ferric chloride in removing turbidity and TOC from Mixture 1 through coagulation – flocculation.



Appendix-Figure 17. Residual turbidity removal as a function of PDADMAC dose for Mixture 1 at pH 3 and 4 (initial turbidity = 33 NTU)



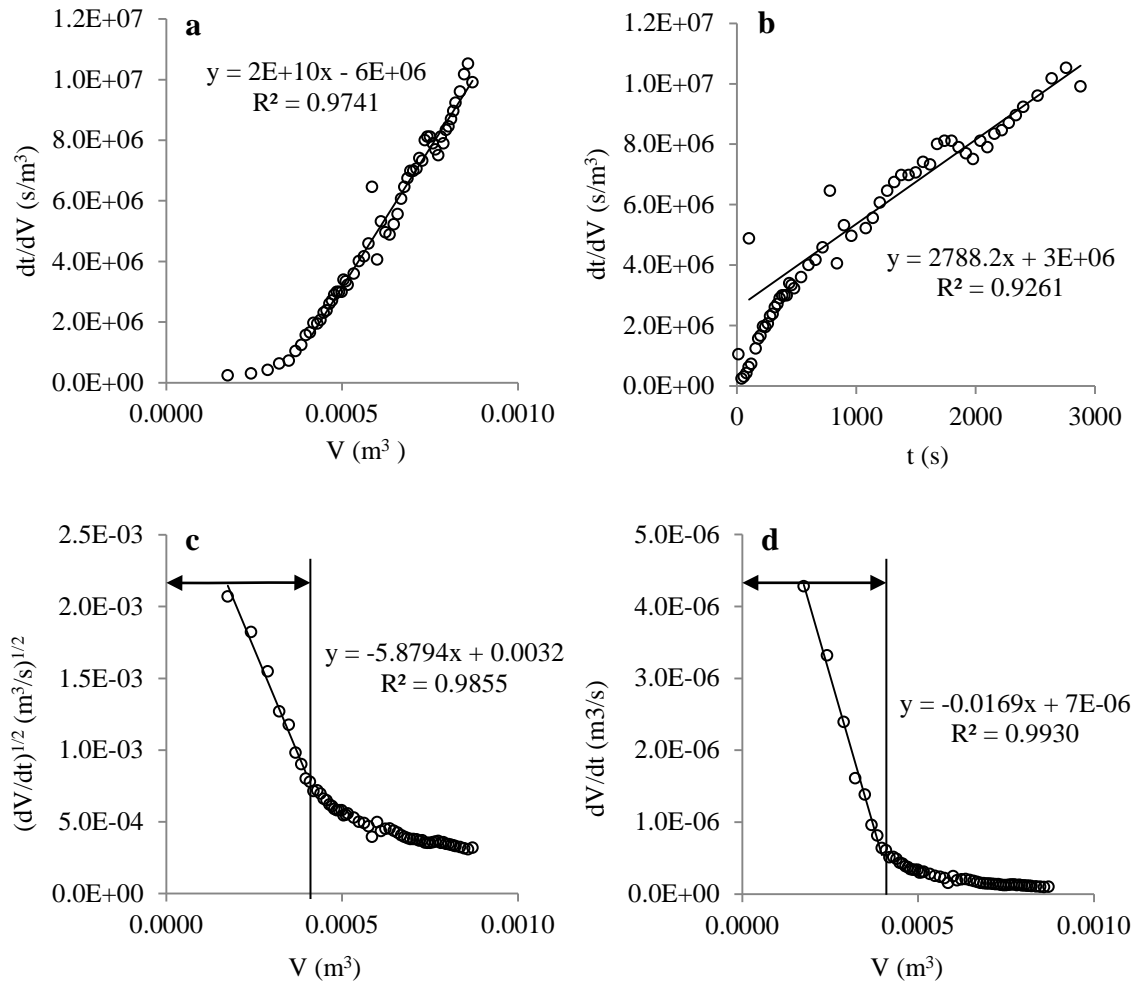
Appendix-Figure 18. Residual turbidity removal as a function of PDADMAC dose for Mixture 1 at pH=4 (initial turbidity = 33 NTU)



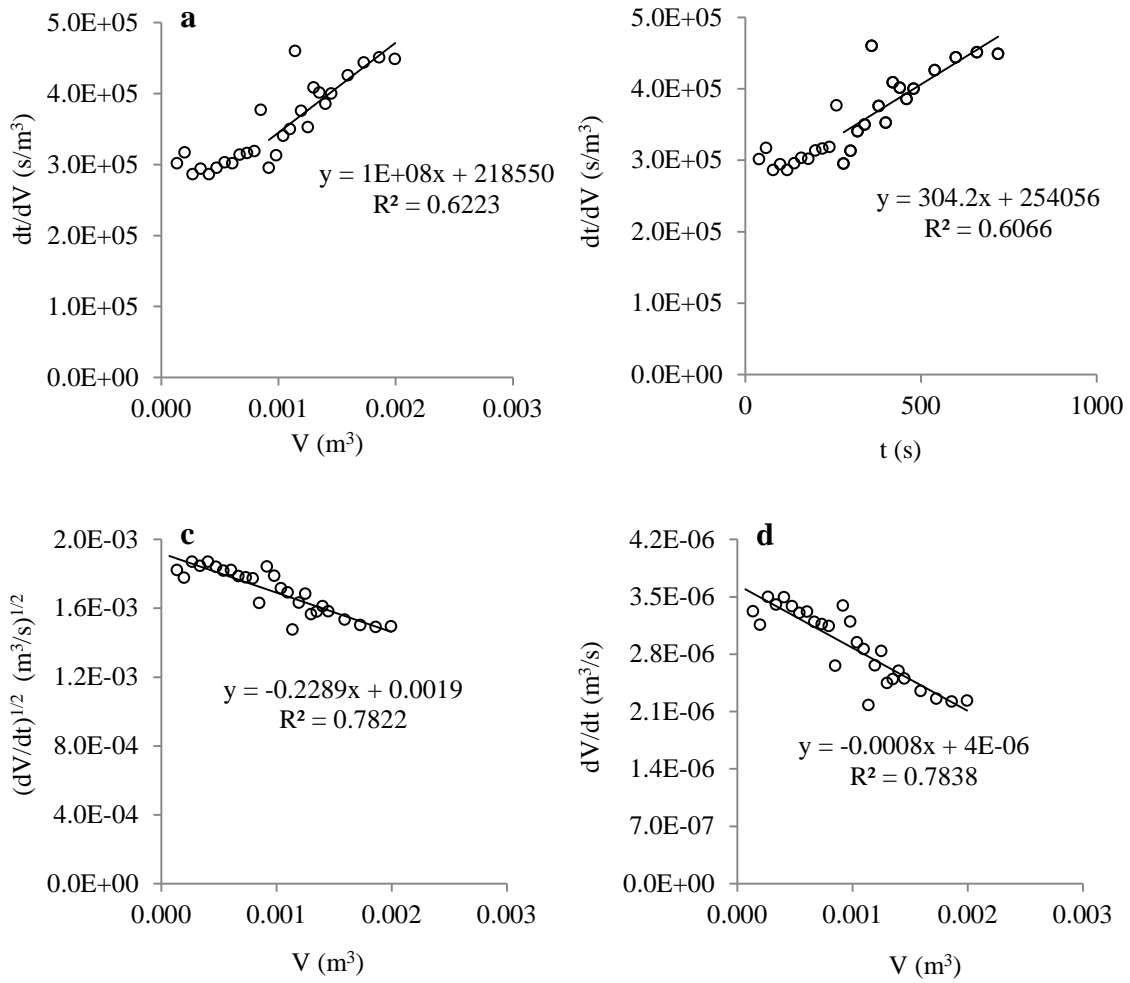
Appendix-Figure 19. Residual turbidity removal as a function of PDADMAC dose for Mixture 1 at pH=3 (initial turbidity = 33 NTU)

APPENDIX C

SUMMARY OF FOULING MECHANISM IDENTIFICATIONS FOR MIXTURE 1 AND MIXTURE 2



Appendix-Figure 20. Fouling mechanism identification for the Mixture 1: (a) Cake filtration, (b) Intermediate blocking, (c) Standard blocking, (d) Complete blocking



Appendix-Figure 21. Fouling mechanism identification for the Mixture 2: (a) Cake filtration, (b) Intermediate blocking, (c) Standard blocking, (d) Complete blocking

BIBLIOGRAPHY

- AlZoubi, H., Rieger, A., Steinberger, P., Pelz, W. Haseneder, R. and Hartel, G. (2010). Nanofiltration of acid mine drainage. *Desalination and Water Treatment*, 21: 148-161.
- Akcil, A. and Koldas, S. (2006). Acid Mine Drainage (AMD): causes, treatment and case studies. *Journal of Cleaner Production*, 14: 1139-1145.
- Arthur, J.D., Bohm, B. and Layne, M. (2008). Hydraulic Fracturing Considerations for Natural Gas Wells of the Marcellus Shale. The Ground Water Protection Council 2008 Annual Forum. Cincinnati, OH, September: 21-24.
- Bonne, P.A.C., Hofman, J.A.M.H. and Hoek, J.P. (2000). Scaling control of RO membranes and direct treatment of surface water. *Desalination*, 132: 109-119.
- Cheng, S., Jang, J., Dempsey, B.A. and Logan, B.E. (2011). Efficient recovery of nano-sized iron oxide particles from synthetic acid-mine drainage (AMD) water using fuel cell technologies. *Water Research*, 45: 303-307.
- Duclos-Orsello, C., Li, W. and Ho, C.C. (2006). A three mechanism model to describe fouling of microfiltration membranes. *Journal of Membrane Science*, 280: 856-866.
- Economides, M.J., Watters, L.T. and Dunn-Norman, S. (1998). *Petroleum Well Construction*. John Wiley & Sons Ltd. West Sussex, England, p: 473.
- EIA. (2011). *World Gas Shale Resources: An Initial Assessment of 14 Regions outside the United States*. United States Information Administration (EIA), April.
- Engelder, T. and Lash, G. (2008). Marcellus Shale Play's Vast Resource Potential Creating Stir In Appalachia. *American Oil & Gas Reporter*, May.
- Gaudlip, A.W., Paugh, L.O. and Hayes, T.D. (2008). Marcellus Shale Water Management Challenges in Pennsylvania. 2008 SPE Shale Gas Production Conference. Fort Worth, Texas, U.S.A., 16-18 November.
- Grace, H.P. (1956). Structure and performance of filter media. I. The internal structure of filter media. *AIChE J.*, 2: 307-315.

- Grenier, A., Meireles, M., Aimar, M. and Carvin, P. (2008). Analysing flux decline in dead-end filtration. *Chemical Engineering Research and Design*, 86: 1281-1293.
- GWPC and ALL. (2009). *Modern Shale Gas Development in the United States: A Primer*. National Energy Technology Laboratory U.S. Department of Energy. Ground Water Protection Council and ALL Consulting.
- Hermia, J. (1982). Constant pressure blocking filtration laws. Application to power-law non-Newtonian fluids. *Trans. I. Chem. E*, 60: 183-187.
- Howe, K.J. and Clark, M.M. (2002). *Coagulation pretreatment for membrane filtration*. AWWA Research Foundation and American Water Works Association.
- Kargbo, D.M., Wilhelm, R.G. and Campbell, D.J. (2010). Natural Gas Plays in the Marcellus Shale: Challenges and Potential Opportunities. *Environmental Science & Technology*, 44 (15): 5679-5684.
- Kidder, M., Palmgren, T., Ovalle, A and Kapila, M. (2011). Treatment options for reuse of frac flowback and produced water from shale. *Industry Report/ Produced Water Society*, 232 (7).
- Kleinmann, R. L. P., Crerar, D. A. and Pacelli, R. R. (1981). Biochemistry of Acid Mine Drainage and a Method to Control Acid Formation. *Mining Engineering*, 33: 300-306.
- Milici, R.C. and Swezey, C.S. (2006). *Assessment of Appalachian Basin Oil and Gas Resources: Devonian Shale-Middle and Upper Paleozoic Total Petroleum System*. United States Geological Survey. Open-File Report Series, 2006: 1237.
- Nordstrom, D.K. (1982). Aqueous pyrite oxidation and the consequent formation of secondary minerals in: *Acid Sulfate Weathering*. Soil Society of America, p: 37-56.
- Pennsylvania Department of Environmental Protection (PADEP). (2010). *PADEP Oil & Gas Reporting Website*. Pennsylvania Department of Environmental Protection. Bureau of Oil & Gas Management, Harrisburg, PA.
- Rahm, B.G. and Riha, S.J. (2012). Toward strategic management of shale gas development: Regional, collective impacts on water resources. *Environmental Science & Policy*, 17: 12-23.
- Reinicke, A., Rybacki, E., Stanchits, S., Huenges, E. and Dresen, G. (2010). Hydraulic fracturing stimulation techniques and formation damage mechanisms - Implications from laboratory testing of tight sandstone - proppant systems. *Geochemistry*, 70 (3): 107-117.
- Reynolds, T.D. and Richards, P.A. (1995). *Unit operations and processes in environmental engineering*. 2nd ed. PWS Publ., Boston.
- U.S. Environmental Protection Agency. (2011). *Final 2010 Effluent Guidelines Program Plan*.

- Viessman, W. and Hammer, M.J. (1985). *Water Supply and Pollution Control*. 4th Edition. Harper & Row Publishers, New York.
- Zhong, C.M., Xu, Z.L., Fang, X.H. and Cheng, L. (2007). Treatment of acid mine drainage (AMD) by ultra-low-pressure reverse osmosis and nanofiltration. *Environmental Engineering Science*, 24 (9): 1297-1306.
- Zularisam, A.W., Ismail, A.F. and Salim, R. (2006). Behaviours of natural organic matter in membrane filtration for surface water treatment—a review. *Desalination*, 194: 211-231.